Adaptive Full Aperture Wavefront Sensor Study

Final Report

Period of Grant: 1 April 1995 to 31 Aug 1997

Grant Number: NAG8-1138

Prepared

by

William G. Robinson, Principal Investigator

Electro-Optics, Environment, and Materials Laboratory
Georgia Tech Research Institute
Georgia Institute of Technology
Atlanta, Georgia 30332

Adaptive Full Aperture Wavefront Sensor Study

Table of Contents

Adaptive Full Aperture Wavefront Sensor Study

1.0 Introduction.

This final report describes the work performed by Georgia Tech Research Institute during the period of 1 April 1995 to 31 August 1997, under Grant No. NAG8-1138. This grant and the work described was in support of a Seven Segment Demonstrator (SSD) and review of wavefront sensing techniques proposed by the Government and Contractors for the Next Generation Space Telescope (NGST) Program.

A team developed the SSD concept. The team involved personnel from NASA Marshall Space Flight Center (MSFC), Naval Air Warfare Center-Weapons Division (NAWC-WPNS), SY Technologies (SYT), Blue Line Engineering (BLE), and Georgia Tech Research Institute (GTRI). The Program Manager for the effort was Mr. E. (Sandy) Montgomery at MSFC. For completeness, some of the information included in this report has also been included in the final report of a follow-on contract (H-27657D) entitled "Construction of Prototype Lightweight Mirrors".

The original purpose of this GTRI study was to investigate how various wavefront sensing techniques might be most effectively employed with large (>10 meter) aperture space based telescopes used for commercial and scientific purposes. However, due to changes in the scope of the work performed on this grant and in light of the initial studies completed for the NGST program, only a portion of this report addresses wavefront sensing techniques. The wavefront sensing techniques proposed by the Government and Contractors for the NGST were summarized in proposals and briefing materials developed by three study teams including NASA Goddard Space Flight Center, TRW, and Lockheed-Martin. In this report, GTRI reviews these approaches and makes recommendations concerning the approaches.

The objectives of the SSD were to demonstrate functionality and performance of a seven segment prototype array of hexagonal mirrors and supporting electromechanical components which address design issues critical to space optics deployed in large space based telescopes for astronomy and for optics used in spaced based optical communications systems. The SSD was intended to demonstrate technologies which can support the following capabilities;

- Transportation in dense packaging to existing launcher payload envelopes, then deployable on orbit to form a space telescope with large aperture.
- Provide very large (>10 meters) primary reflectors of low mass and cost.
- Demonstrate the capability to form a segmented primary or quaternary mirror into a quasi-continuous surface with individual subapertures phased so that near diffraction limited imaging in the visible wavelength region is achieved.
- Continuous compensation of optical wavefront due to perturbations caused by imperfections, natural disturbances, and equipment induced vibrations/deflections to provide near diffraction limited imaging performance in the visible wavelength region.
- Demonstrate the feasibility of fabricating such systems with reduced mass and cost compared to past approaches.

While the SSD could not be expected to satisfy all of the above capabilities, the intent was to start identifying and understanding new technologies that might be applicable to these goals.

2.0 Scope of Work.

The original purpose of this GTRI study was to investigate how various wavefront sensing techniques might be most effectively employed with large (>10 meter) aperture space based telescopes used for commercial and scientific purposes and to develop risk-reduction prototypes, in selected areas, to minimize development risks of future investigators. However, due to changes in the scope of the work performed on this grant and in light of the initial studies completed for the NGST program, only a portion

of this study addressed wavefront sensing techniques. The wavefront sensing techniques proposed by the Government and Contractors for the NGST were summarized in proposals and briefing materials developed by three study teams including NASA Goddard Space Flight Center, TRW, and Lockheed-Martin. In this report, GTRI reviews these approaches and makes recommendations concerning the approaches.

The original statement of work for this contract is shown in Appendix A. Changes in the original scope of work were made in consultation with the COTR (E. Montgomery) in an effort to meet the technical goals of the SSD; schedule constraints presented by the program, and cost limitations of this grant. This report describes the actual work completed on this grant.

3.0 SSD Top-Level Technology Demonstration Requirements.

The following list of top-level technology demonstration requirements was taken from the Seven Segment Demonstrator Project Plan, Revision 2;

The goal of the SSC is to demonstrate:

- Phase locking of a segmented mirror surface.
- Compact (miniaturized) phase loop controller capable of continuous phasing mirrors at a bandwidth in excess of 300 Hz.
- Compact (miniaturized) phase loop controller architecture expandable to many more segments and a tip/tilt control loop for full aperture wavefront correction.
- Miniaturized, high accuracy, high dynamic range edge sensors.
- Miniaturized, high accuracy, high dynamic range, moderate bandwidth, and lightweight actuators.
- Very lightweight mirror segments.
- Simple, reliable, robust construction and deployment methods and mechanisms.
- Stiff cluster baseplates for support of segmented mirror arrays.

The SSD component developments were treated as a precursor to constructing a much larger curved aperture made up of many more segments.

The guidelines and assumptions developed to serve as hardware and software requirements for the SSD were documented in the Seven Segment Demonstrator Project Plan, Revision 2. These requirements are included in this report in Appendix B.

4.0 Magnetic Edge Sensor Development.

The mirrors in the SSD are used to form a quasi-continuous surface, with minimal wavefront deviation. To make the seven smaller segments form a continuous surface like one large mirror; the edges of the segments must match in tilt and piston (displacement). The relative position of the edges of the hexagonal mirrors segments are measured using edge sensors and this relative position is used as feedback for the servo control system. The edge sensors must have the following properties;

- Large positional dynamic range (+/- 200 μm or larger)
- Good resolution (<4 nm rms or less)
- Fairly low non-linearity (1% or less of range)
- Good frequency response (10 kHz or higher)

Magnetic position sensor developed by Kaman Aerospace on an Air Force program called PAMELA met the above requirements, but were difficult and expensive to produce in large quantities. The SSD program goal was to develop a magnetic sensor similar to the Kaman sensor, but less expensive.

4.1 Background.

Prior to GTRI joining the SSD development team, BLE and SYT developed a magnetic position sensor concept to meet the requirements listed above. The original SSD edge sensor design included two integrated circuit die, each one mounted on adjacent edges of a mirror as shown in Figure 4.1-1.

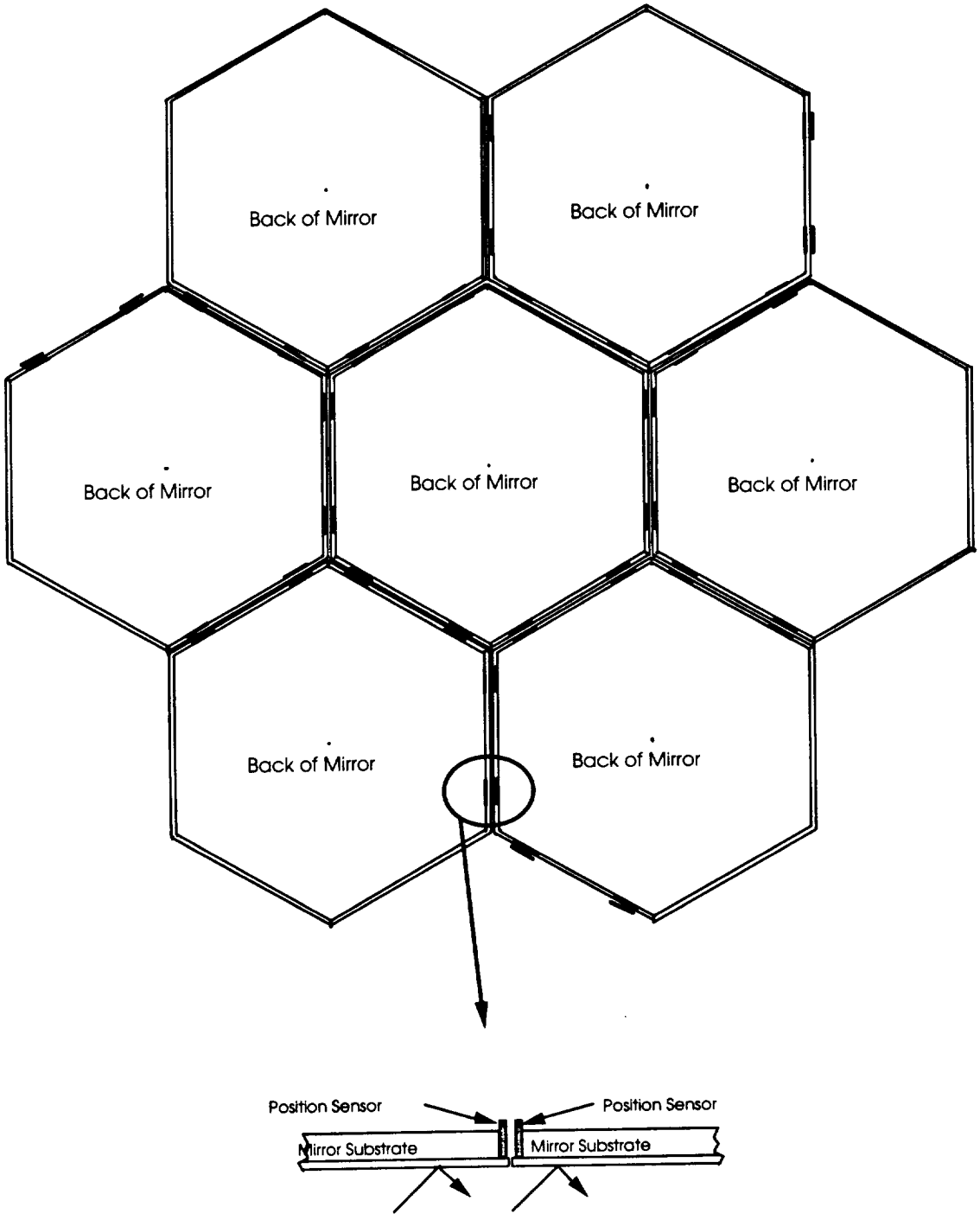

Figure 4.1-1 Schematic of SSD showing position sensors on adjacent mirror edges.

As originally envisioned, each edge sensor circuit had the identical layout, but were interconnected differently depending on its use as a passive or active element. Each sensor pair has one passive coil pair and one active coil pair. The sensor circuit, shown in Figure 4.1-2, contains (1) pads for connection of two coils, (2) drive/oscillator circuitry, (3) and an array of electrical interconnect pads. In the original sensor concept, two coils were to be attached to each circuit and the interconnect pads were to be configured using external bond wires and flex circuitry as shown in Section 4.4.

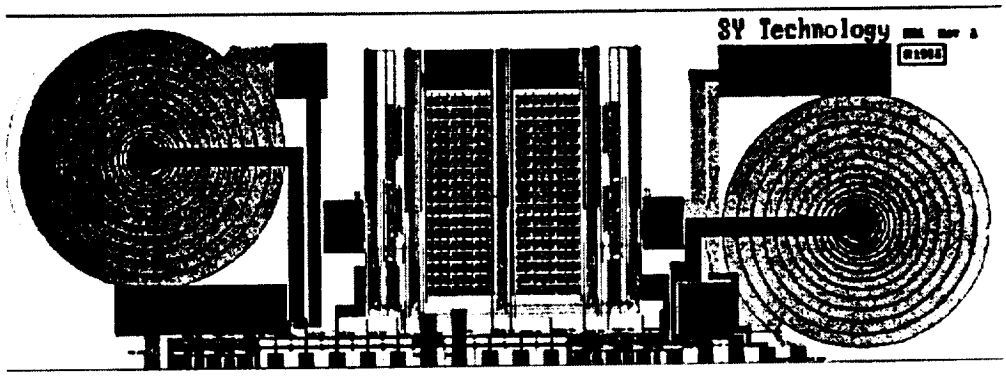

Figure 4.1-2 Position sensor circuit.

4.2 CMOS Sensor Procurement.

The sensor circuit was designed by SYT and fabricated by the MOSIS Fabrication Service. The circuits were fabricated with two circuits per die as shown in Figure 4.2-1 .

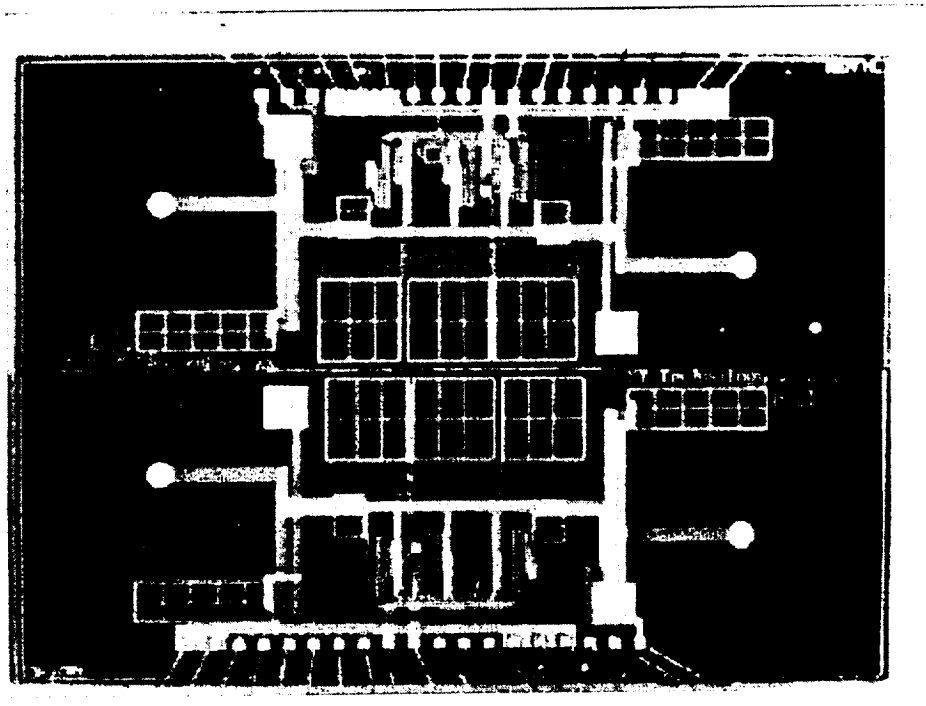

Figure 4.2-1 Photograph of position sensor die showing two identical sensors on the same die.

A total of 44 die (88 sensor circuits) were purchased by GTRI from the MOSIS Fabrication Service. GTRI also had the task of dicing the die into two separate die, each containing one sensor circuit. The MOSIS Fabrication Service is a service offered by the University of Southern California, acting through its Information Sciences Institute, which provides a means of obtaining relatively low cost prototyping and small volume production of custom and semi-custom VLSI circuits. Available processing include the following technologies;

2.0 micron CMOS (Analog, NPN transistor, 2 Poly)
1.2 micron CMOS (Analog, NPN transistor, 2 Poly)
1.2 micron CMOS (Digital w/capacitor option)
0.8 micron CMOS (Digital)
0.5 micron CMOS (Digital)
0.8 micron GaAs (Digital).

MOSIS provides this service by combining designs from various users onto one mask set and then contracting with major commercial IC vendors to fabricate the circuits. Once the wafers are fabricated, MOSIS cuts the wafer into individual die and sends the die to the user or the individual chips can be packaged (including wire bonding) by MOSIS in a number of standard commercial packages. The MOSIS Service has a web site at www.isi.edu and can be reached by telephone at 310-822-1511.

4.3 Magnetic Coil Fabrication

The small coils to be used with the circuits were required to have more inductance than is feasible with normal integrated circuit processing techniques so a special process was employed to fabricate the coil pairs. The coils were produced by the North Carolina Micro-machining Center (NCMC), using the LIGA process. The LIGA process is capable of producing miniature nickel coils that have a thickness-to-width ratio of 4 or 5 to 1 with very straight walls. This allowed the small coils to have the inductance necessary for this application. The LIGA coils are shown in Figure 4.3-1.

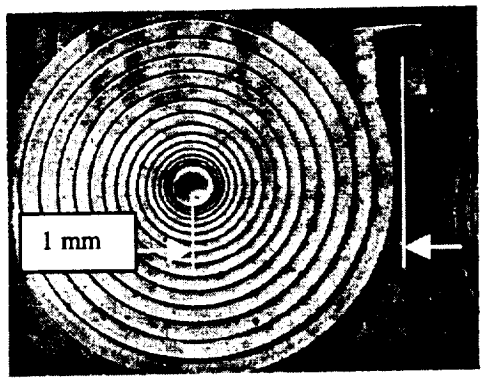

Figure 4.3-1 Photograph of small coils made with LIGA process.

The more traditional way of producing similar coils in the past was by actually winding the coils with special wire on special bobbins. The previous technique was very labor intense, time consuming, and produced low yields due to assembly problems.

4.4 Flex Circuit and Edge Sensor Packaging Design

Several edge sensor packaging concepts were developed which used the position sensor dies, LIGA coils, and flex-circuits provided by NASA Ames. One of the key components to all of the concepts was the flex circuits used to interconnect the position sensors mounted on the edge of the mirrors with the electronics used to control the mirror actuators. Several commercial companies were contacted to determine the suitability of standard products, but all of the "off-the-shelf" products found were unsuitable for this application and custom products were too expensive for our budget. Prior to GTRI's participation in this program, SYT had discussed with NASA Langley Research Center the possibility of using a new polyimide material they had developed called LaRC-SI. LaRC-SI is a polyimide type of material, which can be laid down in very thin layers, which allows for a very flexible membrane with good electrical properties. When GTRI joined the program and it became GTRI's responsibility to provide edge sensor packaging designs, Nancy Holloway, at Langley Research Center, was contacted to further investigate how various flex circuits might be developed.

Early flex circuit designs had eight traces, as shown in Figure 4.4-1, to accommodate all of the power and signal connections required to operate the sensor circuit. Initial concepts used wire-bonding between circuit pads on the silicon die to circuit pads on the polyimide flex circuits, as shown in Figure 4.4-2.

Figure 4.4-1 Early flex-circuit showing 8 traces

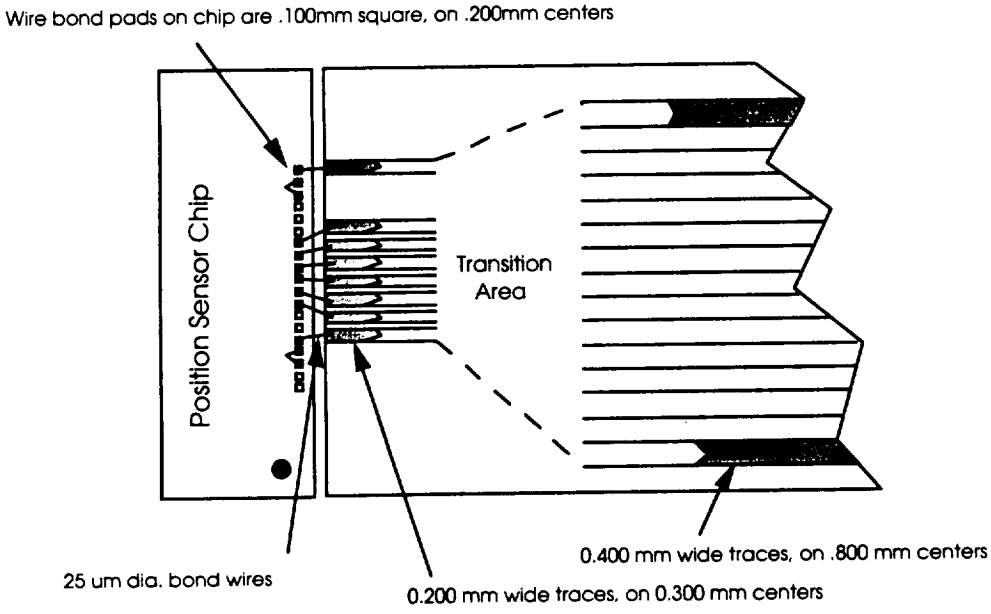

Figure 4.4-2 Early sensor-flexcircuit interconnect design

For various reasons, these concepts proved to be too labor intense (expensive), too fragile, or required special bonding equipment that was not standard in the industry. GTRI finally settled on the design shown in Figures 4.4-3 and 4.4-4.

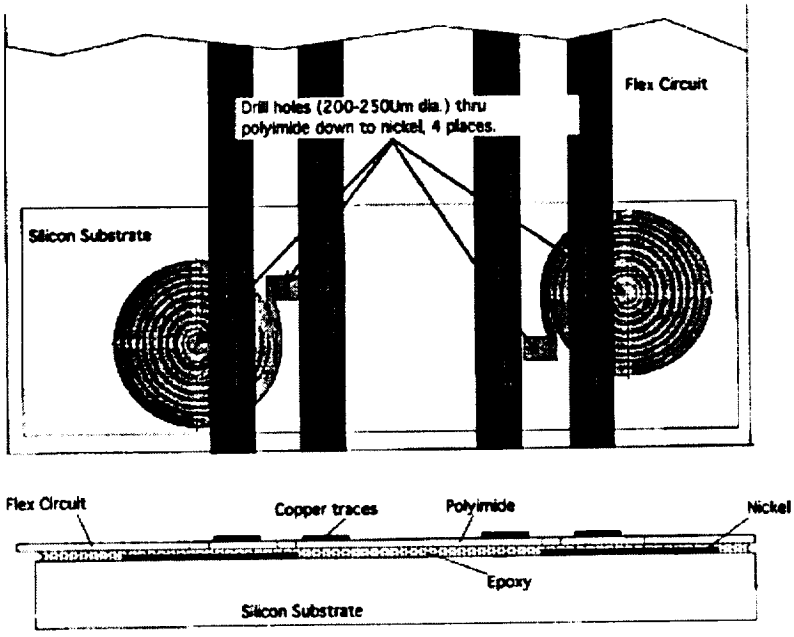

Figure 4.4-3 Final sensor-flex circuit interconnect design

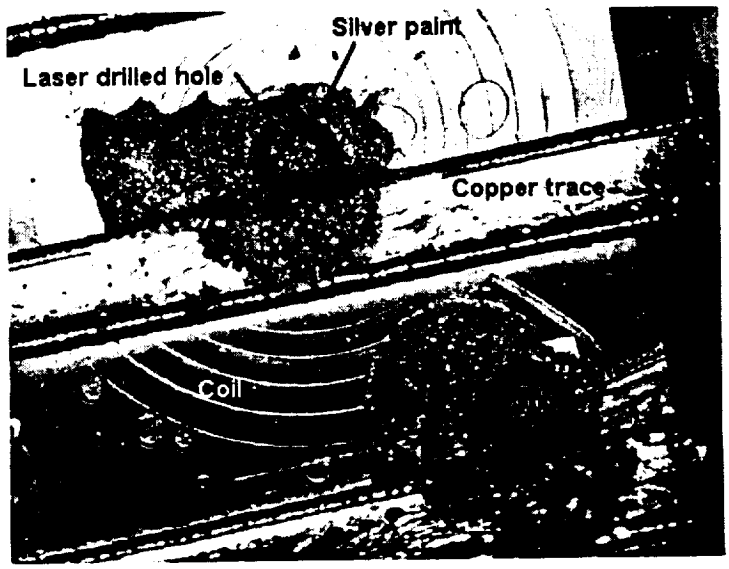

Figure 4.4-4 Photograph of final bonding technique.

This design is simple, robust (does not require fragile wire bonds), and allows a large number of prototype packages to made fairly quickly using simple fixturing. Details of this packaging scheme are described in the final report entitled "Construction of Prototype Lightweight Mirrors" on Contract H-27657D.

5.0 Optical Position Sensors.

As a parallel risk reduction effort, optical position sensor concepts were considered. During this short study a number of designs were identified through a literature search. The literature search provided the following interesting concepts;

5.1 Young's Double Slit Interferometer.

A paper by C.W. Gillard, et al [1] describes a form of Young's double slit interferometer using an light emitting diode and white light source that allows measurement of (1) relative piston between two mirror segments, (2) the gap between the segments, and (3) the relative tilt between the segments. The technique is reported to give piston accuracy (rms) of 0.013 μm, gap accuracy (rms) of 1.6 μm, and tilt accuracy of 0.02 arc sec (110 nrad). This approach uses a CCD array as a readout device. From a packaging standpoint, one major advantage that this technique has is that all of the electronics are located off the segments on the backup structure.

5.2 Laser Diode Optical Feedback Displacement Sensors.

Three papers were found that describe the use of external cavities with the Fabry-Perot cavities of laser diodes to produce modulation of the laser diode output as a result of changes in the external cavity position. The paper by J. Kato, et al [2] describes a technique that allows displacement measurement accuracy of +/- 100 nm over a range of 1mm. Another paper by P. de Groot [3] describes a similar experiment using external laser diode cavities to measure displacements of a piezo-electric driven mirror. The third paper by J. Remo [4] describes, in a more theoretical way, analysis of external cavity laser diode based edge sensors. In this paper the external cavity is defined by a calibrated diffraction grating.

5.3 Integrated Optics Michelson Interferometer (IOMI).

Two papers by John Remo [3] describe the selection and use of externally coupled and internally placed laser diodes in an integrated optics chip utilizing a Michelson interferometer design. The papers specifically address the use of this type of integrated optic device for piston and tilt measurements of segmented mirror reflectors for power beaming applications. The results indicate that the prototype "can provide precise distance measurements from 20 nm to a few millimeters with a very small standard deviation" (1.2-1.8 nm) and tilt measurements from 1 to about 100 micro-radians.

5.4 Integrated-Optic Interferometer Position Sensor (IOPS).

This paper by Shogo Ura, et al [4] describes an integrated optics device that includes two planar interferometers, two photodetectors, an externally coupled laser diode, and three types of grating structures to couple laser energy to an externally movable mirror and provide the reference beams for the interferometer. The author reports a measurement resolution of about 10 nm can be achieved, provided a stable laser wavelength. Mirror-to-sensor range of up to 15 cm provided high enough visibility to obtain the 10 nm resolution. The unique part of this device is the use of various grating structures in the design and of course the large apparent dynamic range.

5.5 Absolute Displacement Sensor Using Moiré Fringe Techniques.

This paper by Barry Jones and Graeme Philp [5] describes a technique for using fiberoptics and gratings to produce a displacement sensor based on Moiré fringe effects. The heart of the system is a four channel "interpolator" to measure the phase angle of the fringes. The prototype sensor described is usable over a range of 100 um, with a resolution on the order of 12 nm. The author also discusses a multi-wavelength sensor using wavelength multiplexing to reduce the number of fiberoptics required to operate the sensor.

Due to a lack of schedule time, none of the above optical techniques were pursued. However, the area of optical position and tilt sensing may be a fruitful area to pursue in future studies. While many of the optical position sensing techniques have been implemented in an integrated-optics format, the implementations are still being developed and more devices need to be constructed and tested under different environmental and operational conditions. Until more of the techniques are used in a systematic testing program, their subtle faults will not be uncovered. In conclusion, the approach shows a lot of promise, but needs a lot of work to understand where and how it might be successfully implemented.

6.0 Wavefront Sensing Techniques for the Next Generation Space Telescope.

As stated in section 2.0, Scope of Work, one of the tasks in the revised statement of work included a review of wavefront measurement techniques that were proposed by the three NGST design teams. This review is presented in report format in Appendix C.

The review, by Dr. Haken Urey, discusses the wavefront sensing techniques proposed by the Goddard Space Flight Center team, the TRW led team, and the Lockheed-Martin led team. The report also discusses the theory behind the proposed wavefront sensing techniques (with references) and offers recommendations.

7.0 Conclusions.

7.1 Edge Sensors.

The initial packaging designs, which used wire bonds to electrically connect the full complement of outputs/inputs from the silicon sensor circuit pads to the flex-circuit pads, suffered the following problems;

- Assembly of the various components and wire bonds was too labor intense, which would result in high assembly costs.
- The number of parts and assembly steps would require a great deal of time to complete the assemblies.
- The wire bonds are very fragile and problematic during handling and assembly of the sensors to the mirrors and during handling and assembly of the mirror segments into the SSD.
- Using eight traces on the flex-circuit increased the stiffness of the flex-circuit more than desired.
- Having most of the oscillator/drive circuitry for the coil on the sensor die, produces heat at a location which is difficult to remove except through heating of the mirror.

These potential problem areas, coupled with the fact that the sensor circuits did not operate properly, led to a new design concept and implementation of the new concept in the follow-on contract discussed previously in Section 1.0.

Several optical position sensing techniques seem to show promise in meeting the requirements of edge sensing. However, until prototypes of these concepts are constructed and integrated into the overall design of a mirror control system, it will be difficult to determine some of the subtle problems associated with these new designs.

7.2 Wavefront Sensing for NGST.

Intensity-based wavefront sensing techniques (phase retrieval, phase diversity, prescription retrieval, and curvature sensing) show potential without much additional cost. One of the primary

advantages of these techniques is that they can, to some degree, be adaptable to the level of correction required. However, one of the big unknowns at this time, is how much data will be required for various wavefront solutions, the bandwidth requirements, and where the calculations will be performed?

8.0 Recommendations.

8.1 Edge Sensors.

It is recommended that any edge sensing scheme, either magnetic or optical, should minimize the amount of circuitry and heat generated on the mirror substrate. In addition, the mirror substrate and sensor should be designed concurrently with the requirements of both being considered as an integrated package.

While it appears that an optical sensing technique might have an advantage in meeting more of the overall system requirements compared to the magnetic type of sensor, it is difficult to be certain without additional prototyping and testing. It is therefore recommended that a promising optical position sensing technique be developed that is consistent with the overall design requirements of the segments and that a prototype of the sensor be designed, fabricated, integrated, and tested.

8.2 Wavefront Sensing for NGST.

All of the wavefront sensing techniques proposed by the NGST concept design study teams have the possibility of meeting the speed, accuracy, and dynamic range requirements of NGST. Therefore, it is important that the appropriate technique concentrate on meeting the other requirements of hardware and software reliability, ease of alignment, spectral range, and development costs.

It is recommended that further trade studies be performed, concurrently with the telescope design and operational scenarios, to further define how the proposed approaches compare. A down selection should be made to the two best designs and these designs should be prototyped and tested. Extensive testing should be carried out here on earth, but also in space.

9.0 Acknowledgments.

The author would like to acknowledge the expertise and help supplied by Mr.Stan Halpren in dicing the sensor circuits and coil pairs and also in packaging the test circuits which required a considerable number of wire bonds. Dr. Haken Urey is acknowledged for his review and discussion of the wavefront sensing techniques proposed for the NGST. The author would also like to thank Sandy Montgomery, the NASA Marshall Program Manager; Greg Ames of Blue Line Engineering; John Karpinsky of SY Technologies; and Don Decker of Naval Air Warfare Center for their participation in technical discussions and helpful suggestions. And certainly, a great deal of thanks goes to NASA MSFC for the funding that allowed us to explore some of the technologies and processes described in this report.

10.0 References for Section 5.0

[1] C.W. Gillard et. al., "Segmented mirror edge alignment sensor", SPIE Vol. 444, pp. 310-318, 1983.

[2] J. Kato et. al., "Optical feedback displacement sensor using a laser diode and it performance improvement", *Measurement Science and Technology*, Vol. 6, pp. 45-52, 1995.

[3] Peter de Groot, "Applications of optical feedback in laser diodes", *Laser Diode Technology and Applications II*, SPIE Vol. 1219, pp. 457-467.

[4] John L. Remo, "Laser diode edge sensors for adaptive optics segmented arrays Part 1: External cavity coupling and detector currents", *Laser Power Beaming*, SPIE Vol. 2121, pp. 83-90, 1994.

[5] John L. Remo, "Laser diode edge sensors for adaptive optics segmented arrays Part 2: Laser diode coupled integrated optics chip", SPIE Vol. 2376, pp. 188-199, 1995.

[6] John L. Remo, "Semiconductor diode laser coupling to integrated optics", SPIE Vol. 2383, pp. 211-223, 1994.

[7] Shogo Ura et. al., "Integrated-optic interferometer position sensor", *Journal of Lightwave Technology*, Vol. 7, No. 2, pp. 270-273, 1989.

[8] Barry E. Jones et. al., "An absolute displacement sensor using moiré fringe techniques with multimode optical fibers", *Fiber Optics '85*, SPIE Vol. 522, pp. 184-195, 1985.

Appendix A: Statement of Work

Statement of Work
for an
Adaptive Full Aperture Wavefront Sensor (AFAWS) Study

1.0 Introduction

A program of technology development and advancement efforts is going on under the joint sponsorship of NASA and the US Navy to (1) retain leadership in electro-optics, (2) perform applied optics for civilian, defense, and commercial purposes, and (3) advance technologies that will drive major civilian commercial development opportunities. The name of the program is National Advanced Optics Mission Initiative (NAOMI). One of NASA's technology efforts under the NAOMI program umbrella has as its goal to produce a 12 meter aperture segmented primary mirror, simple Cassegrain, optical ground-based telescope with adaptive compensation capabilities. The telescope is named ATTILA for Advanced Technology Telescope, Integrated Large Aperture.

One of the major subsystems of ATTILA is a wavefront sensor required to sense the relative phase of the optical wavefront, so that the primary mirror can correct for perturbations caused by all expected sources including surface distortions due to inertial flexure and thermal changes. For the purpose of this proposal the wavefront sensor is referred to as the Adaptive Full Aperture Wavefront Sensor (AFAWS). The AFAWS samples the distorted full aperture wavefront produced by the telescope optics, determines telescope segment corrections required to produce a plane wavefront, and provides these corrections to the ATTILA control system in a format most useful for overall system performance. The AFAWS must interface optically, mechanically, thermally, and electrically (power and signal) with the ATTILA system. This interface must include any metrology elements needed for the system to meet the overall system requirements. The AFAWS subsystem must also meet schedule and cost objectives of the program.

This proposal describes a study to establish requirements and investigate concepts for an Adaptive Full Aperture Wavefront Sensor (AFAWS). The intent of the study is to validate an AFAWS concept that is fully scalable and that is cost effective for a subsystem having 10^5 or more channels. The following tasks are structured to begin immediately and conclude with the end of the current phase II program. This study shall provide the necessary foundation to support a Phase B preliminary design review in the area of wavefront sensing.

Georgia Tech Research Institute personnel have the experience and background to complete this proposed study in a manner that is beneficial to MSFC. The Principal Investigator for this study, William Robinson, has 14 years experience at the National Optical Astronomy Observatory (NOAO) developing astronomical telescopes and instrumentation. Some of the instrumentation developed by the PI at NOAO was related to optical image recording, with an interest in improving the optical wavefront of the system. The PI also served as Technical Program manager for the sensor subsystem on a joint Air Force/NASA program call Starlab. One of the objectives of the spacebased Starlab mission was to implement wavefront sensing and correction coupled with precision pointing and tracking experiments. The PI also spent 4 years working on classified DoD adaptive optics programs as part of SDIO programs.

In addition to the background of the PI in adaptive optics, other GTRI personnel that would participate in this study have been involved with the developement of high speed, low noise CCD cameras for wavefront sensors. GTRI has developed the fastest, lowest noise CCD camera for astronomical wavefront sensing that is presently available. This camera would be a major component for any type of wavefront sensing architecture. In addition to the development of this CCD camera based on CCDs developed by Lincoln Labs, GTRI has development contracts which involve the development of high speed CCD detectors for the high definition TV market and has access to other high speed CCD detectors being produced by Air Force Phillips Lab for wavefront sensing, when they become available.

GTRI has unique capabilities to produce designs and prototype electro-optical components taking advantage of the personnel and facilities of the Microelectronic Research Center, micro-machine manufacturing facilities, multi-chip module fabrication capabilities, and optical test instrumentation including a Wyko test interferometer. The experienced personnel and related facilities available at Georgia Tech are uniquely applicable to the goals of this study and objectives of MSFC.

2.0 Tasks

The following tasks define the work breakdown structure for this study and are intended to be completed as part of the Statement of Work for the study.

2.1 Requirements definition

Define top-level system wavefront sensing requirements in terms of performance, operational, physical, and environmental parameters. Flow the top-level system wavefront sensing requirements down to AFAWS design requirements. This task will be accomplished with heavy interaction between GTRI and NASA personnel.

2.2 AFAWS Concept Design Development

2.2.1 Identify various optional approaches and develop top-level design configurations for implementation of each approach.

2.2.2 Analyze compliance of each design configuration with performance, operational, physical, and environmental requirements.

2.2.3 Identify the risks (performance, operational, physical, environmental, schedule, cost) with each concept.

2.2.4 Determine the most promising concept design(s).

2.3 Risk Reduction Prototype Hardware Development

Identify and produce prototype hardware to support risk reduction activities of future development. The detail prototyping objectives of this task will be defined by task 2.2.4 and with heavy interaction between GTRI and NASA personnel.

2.4 Final Report

Prepare and present a final report that describes the results of the study.

Appendix B: Seven Segment Demonstration Program Plan

Appendix B: SSD Project Plan, Revision 2

Revision 2

DRAFT

ULTIMA
(Ultra Lightweight Telescope, Integrated Missions for Astronomy)

Segmented Corrector Research

Seven Segment Demonstrator

Project Plan

May 27, 1996

1.0 Introduction and Background

After a visit to PAMELA (Phased Array Mirror, Extendible Large Aperture) telescope demonstrator in the fall of 1994, the NASA administrator directed that the program emphasis be concentrated on space-based telescopes, and that applications in space-based astronomy be pursued with increased vigor. A science team was formed by the University of California, Berkeley, Space Science Laboratory proposed to the NASA Headquarters' Office of Space Sciences the development of an ISSA-based optical observatory using PAMELA derived technology. Although unsuccessful, a core group of proponents have coalesced to continue promoting the effort. Other involved parties include the Space Telescope Science Institute, the Jet Propulsion Laboratory, Langley Research Center, and several other universities and contractors. On March 23, 1995, the NASA associate administrator for the Office of Space Access and Technology directed the evolution of the technology from the laboratory to a space system. The Advanced Concepts Office was tasked with an effort focused toward defining a near term demonstration in space of the key technologies. A development plan was derived encompassing thin membrane mirrors as well as adaptive segmented mirror technologies. A strawman goal of a 20 meter filled aperture at the Earth-Sun L1 point was chosen as the strawman configuration for the ULTIMA (Ultra Lightweight , Integrated Missions for Astronomy.

Coincidentally, The Office of Space Science at NASA Headquarters began studying a potential follow-on to the Hubble Space Telescope. Eventually this effort was combined with a space interferometry program into the Origins Program. The HST follow-on is being called the Next Generation Space Telescope (NGST) and is initially conceived as an 8 meter filled aperture also operating at the Earth-Sun L1 point.

The following plan describes how OSAT-funded FY95 research efforts, SBIR projects, and MSFC discretionary funds are being combined in a project to make the next step in the maturation of active segmented space mirror technology whcih could be of benefit to ULTIMA, NGST, and other NASA advanced optics programs. The name chosen for this effort is the Seven Segment Demonstrator (SSD) project

2.0 Objectives, Requirements, and Scope

2.1 Management Objectives

The management objectives for the Seven Segment Demonstrator program are to demonstrate functionality and performance of a seven segment prototype array of hexagonal mirrors and supporting electromechanical equipment which addresses design issues critical to a space telescope.

2.2 Technology Requirements

The SSD will demonstrate technologies which will support these system capabilities:

(1) to be transported in dense package to fit existing launcher payload envelopes, then construct/deploy to form space telescopes with large apertures,

(2) to continually compensate for image distortions due to imperfections, natural disturbances, and equipment induced vibrations/deflections,

(3) to provide very large primary reflectors of low mass and cost.

(4) to develop the capability to correct spatial and temporal distortions typical of those arising from ambient space environments and from on-board system operations sufficiently to provide near diffraction limited performance,

(5) to demonstrate the ability to form a segmented primary or quaternary mirror into a quasi-continuous surface with individual subapertures phased so that near diffraction limited performance is achieved, and

(6) to demonstrate the feasibility of fabricating such systems with reduced mass and cost over alternate technologies.

The SSD program draws its resources from various sources and through various contract vehicles as show in Figure 1. The project is enabled because MSFC is the lead center for all the constituent efforts (except the uncompensated contributions).

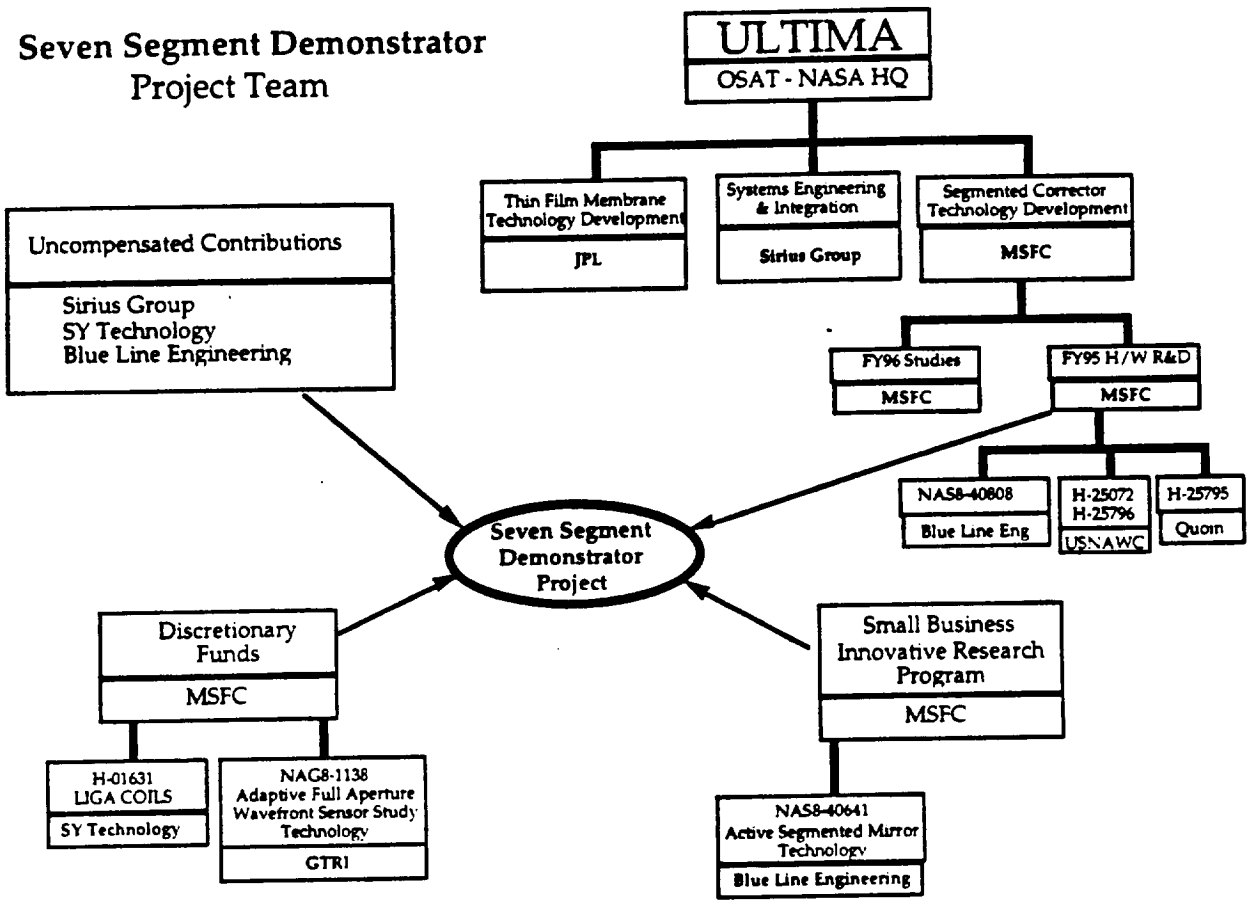

Figure 1. ULTIMA Project Team

2.2 Scope

The scope of the seven segment demo program spans concept development, prototype design, build, integrate, test, and demonstrate. Components of the seven segment demo are a precursor to constructing a much larger curved aperture made up of many more segments. It should demonstrate relevant technologies in:

(1) Phase locking of a segmented mirror surface,

(2) A compact phase loop controller capable of continuously phasing mirrors at a bandwidth in excess of 300 Hz,

(3) A compact controller directly expandable to incorporate many more segments and a tip/tilt control loop for full wavefront correction,

(4) Miniaturized, highly accurate edge sensors,

(5) Miniaturized, highly accurate, lightweight actuators,

(6) Very lightweight mirror faceplates,

(7) Easy, reliable, robust construction/deployment methods and mechanisms, and

(8) Cluster base for the array.

2.3 Guidelines/Assumptions

The following set of guidelines have been established to provide additional focus to the effort

(1) The demonstrator will be designed for monochromatic operation at 632 nm, but is demonstrating a technology path to wavelengths in the range of 500 nm<λ<10 μm,

(2) The main demonstration will be to set the SSD on a table , initialize the mirror segments to an out-of-phase and unaligned condition, then then bring the flat mirror surface into a co-linear, phased condition, and then maintain that condition in the presence of disturbances provided by picking up the array and moving it to several orientations with respect to the local vertical and carefully striking the SSD to simulate impulsive disturbances.

(3) The primary mirror array and segment surface figures will be flat.

(4) The inter-segment gap spacing will be less than 2% of the aperture,

(5) The regular hexagonal segment size will be 7 cm flat to flat,

(6) The demonstrator will operate on 110V AC

(7) SSD Hardware and software will deliverable property to MSFC. Deliverable s will be shipped to:
Transportation Officer, Building 4471
National Aeronautics and Space Administration
George C. Marshall Space Flight Center
Marshall Space Flight Center, AL 35812

(8) There will be eight segments developed for the primary mirror. There array will consist of one center segment plus the first ring of six segments. The eighth segment is a fully completed spare. One segment to be located in the center of the array will have a circular hole in the middle.

(9) A short assessment study will determine the optimum choice between testing an advanced algorithm controller with the seven segment array or a many segment simulator. Until the results are available, the baseline control algorithm for the seven segment array will be simple nearest neighbor. Controller electronics will be miniaturized to the largest extent possible

(10) Edge sensor, actuator, and other data handling electronics will be miniaturized.

(11) A "notebook" computer will serve as the top level host.

(12) The baseline edge sensor technology will be the inductive device developed originally under SBIR by Kaman/Blue Line/SY Technology and lately improved by SY Technology. The fall back position is a simple capacitive gauge mounted beneath the faceplate.

(13) A preliminary layout diagram for the test set-up is shown in figure 2.

(14) It is desired to (A) retain design features for segment phasing, deployment mechanisms, fit, form, and function, of key optical, , and electronic components while (B) accepting design simplifications in place of highly polished mirrors, esoteric materials, NGST optical prescription, thermal management, plasma charging, and bus voltage in order to accomplish the project on time in budget.

(15) Bandwidth of Controller will be 300 Hz.

(16) Edge sensor and, if possible, actuator electronics reduced to application specific integrated circuits (ASICs).

Demonstration System Concept

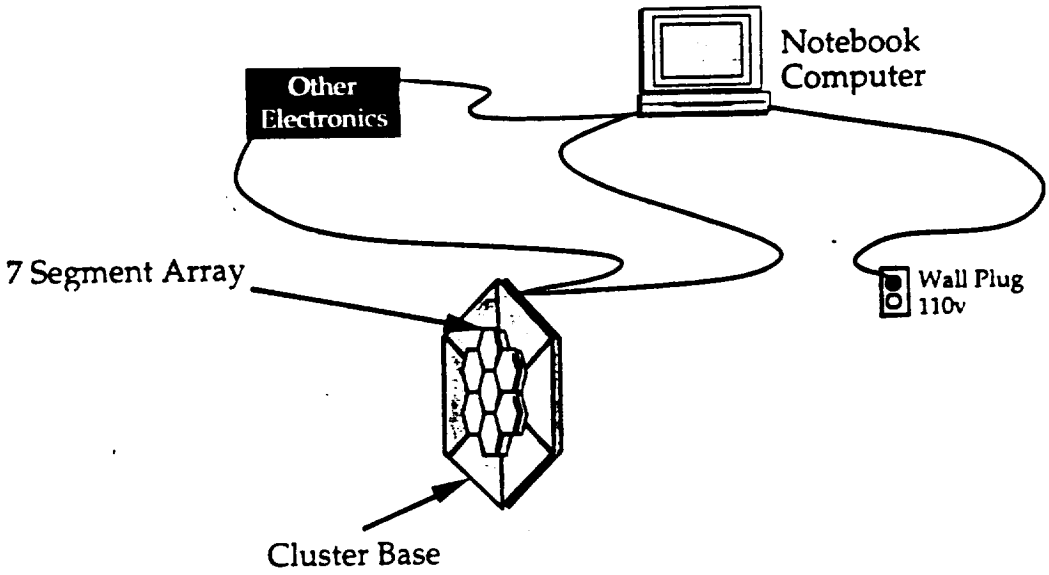

Figure 2. Layout for Demonstrator

3.0 Responsibilities and Interfaces

Roles and responsibilities and a discussion of the major interfaces is provided under bold heading for each participant in the team: MSFC, Blue Line Engineering, USNAWC, GTRI, and SY Technology. In addition, Dr. Glenn Zeiders and Dr. Harold Bennett will be working as general trouble-shooters and consultants for the project. Figure 3 illustrates those relationships.

Marshall Space Flight Center

At MSFC , Sandy Montgomery will be the project manager. He can be reached at (205) 544-1767. His fax number is (205) 544-5861. Henry Waites is the principle investigator over the PAMELA testbed. His phone number is (205) 544-1767. His fax number is (205) 544-5416.

3.1 Project Management

The lead organization for the Seven Segment Demonstrator Project will be Marshall Space Flight Center. Contracted activities of the project team member organizations will be through MSFC and the COTR for those activities is Sandy Montgomery. Periodic reviews to NASA headquarters and MSFC management will be given by MSFC to the management to minimize overhead in the project.

3.2.4.4 Test

As a minimum, MSFC will provide an optical bench in a clean stable environment, access to 110V power, and other basic amenities in support of configuring a test set-up. Subject to availability, MSFC will provide the WYCO 6000 interferometer, LCR meters , auxiliary cameras/monitors, and other auxiliary electrical, optical, and mechanical supporting hardware. MSFC will review the test procedures provided by Blue Line and identify the availability of test-specific government furnished equipment. MSFC will provide one man-level of support to Blue Line for two weeks to configure the SSD in the testbed and run tests. Data results will be analyzed by MSFC and Blue Line.

3.2.4.5 Demonstrations

MSFC will be responsible for developing and providing demonstration briefing materials. MSFC will organize, participate in, and possibly be the sole conductor of potential demonstrations at sites including MSFC, NASA headquarters, GSFC, JPL, and technical conferences and symposia in the United States.

Responsibilities & Interfaces

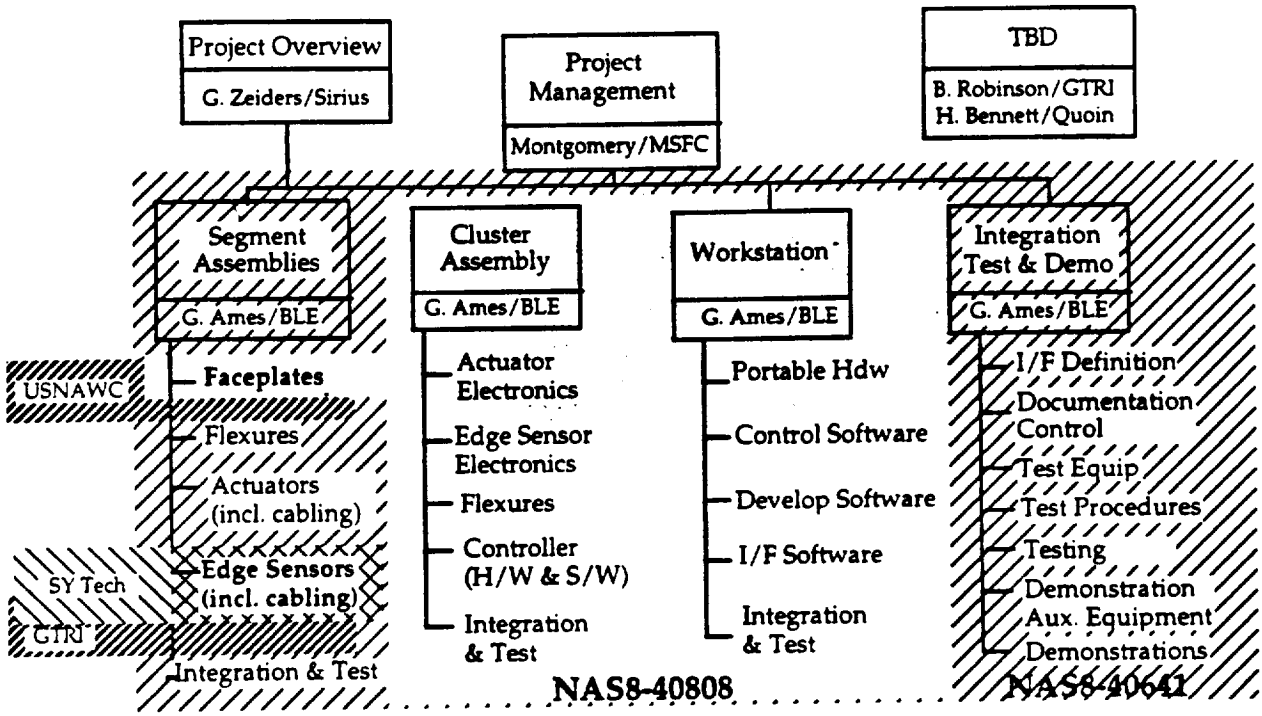

Figure 3. Management Structure

Blue Line Engineering

As shown in figure 3, Blue Line Engineering is responsible for the bulk of the activity. A major portion of the resources for the activity are available as a result of Blue Line's Phase II SBIR program to develop a seven segment demonstrator of 3 cm flat-to-flat size. The SSD elements are "early prototypes" toward the SBIR product. Because of this condition, intellectual property rights to the SSD segments are the same as for the those SBIR segments and must be accordingly protected by the government. Other privately-owned business members of the SSD team will be expected to execute Non-disclosure agreements with Blue Line. This situation does not supersede the intellectual property rights to the inductive sensor technology currently addressed in agreements between Kaman, Blue Line, and SY Technology.

Greg Ames is the lead engineer and project manager at Blue Line. He can be reached at (719) 447-1373. His fax number is (719) 389-0631. Specific responsibilities include:

3.2.1 Segment Assemblies

Blue Line will be responsible for the lead engineer function over all 3.2.4.X activities. Technical and programmatic issues will be identified and reported in a timely manner to NASA. Summary assessments will be given at the design reviews.

3.2.1.1 Faceplates

Blue Line will be responsible for deriving design specifications and delivering them to USNAWC for the eight faceplates.

3.2.1.2 Flexures

Blue Line will be responsible for design, fabrication, test and assembly of 21 flexures for the primary, 3 flexures for the spare mirror segment, and 3 spares for a total of 27 flexures.

3.2.1.3 Actuators

Blue Line will be responsible for design, fabrication ,test and assembly of 21 actuators for the primary, 3 actuators for the spare mirror segment, and 3 spares for a total of 27 actuators.

3.2.1.4 Edge Sensors

Blue Line will assist in the development by providing design review comments on the miniaturized inductive edge sensors to GTRI and SY Technology. Blue Line developed alternate edge sensor technologies will be incorporated into the demonstrator (by Blue Line) at the discretion of Blue Line, i.e. no requirement is levied.

3.2.1.5 Integration & Test

Blue Line will be responsible for providing design coordination information during early stages of the program. Blue Line will receive and inspect edge sensor assemblies from SY Technology and finished and coated mirror faceplates from USNAWC. Blue Line will develop segment assembly procedures and tooling, Blue Line will plan, integrate, and execute appropriate functional tests for the segment assemblies. Blue Line will deliver segment assemblies for integration to the cluster assembly (3.2.2.5 below).

3.2.2 Lead Engineer for Cluster Assembly

Blue Line will be responsible for the lead engineer function over all 3.2.2.X activities. Technical and programmatic issues will be identified and reported in a timely manner to NASA. Summary assessments will be given at the design reviews.

3.2.2.1 Structure

Blue Line will be responsible for design, fabrication ,test and assembly of the supporting structural element for the seven primary mirror segment assemblies(3.2.1.5). As much as possible, the cluster assembly should demonstrate desirable features of robust deployability, lightweighting, and low temperature operation.

3.2.2.2 Controller (H/W & S/W)

Blue Line will be responsible for developing the design of the central computational engine for the segment control algorithm and data management needed to receive error signals from (the wavefront error sensor system if one existed and) the segment edge sensors, interpret them and use the information to set piston commands for the segment actuators in a closed loop control system such that the array mirrors will be positioned to achieve the specified WFE and bandwidth. Blue Line will be responsible for the design, fabrication , test and assembly of the appropriate cluster-level hardware and software in this task.

Blue Line will be responsible for providing to GTRI the cluster-side interface definition necessary for GTRI to develop the cluster assembly-to-edge senor electronics power and data interface hardware.

3.2.2.3 Actuator Electronics

Blue Line will be responsible for design, fabrication ,test and assembly of 21 sets of actuator drive electronics for the primary, 3 sets for the spare mirror segment, and 3 spares sets for a total of 27 sets of actuator drive electronics. Reduction in size of the electronics will be a important design feature. Applications specific integrated circuits will be used wherever possible. Blue Line will trade-off locating the circuits on the segment or cluster assemblies, then implement the preferred approach.

3.2.2.4 Edge Sensor Electronics

Blue Line will be responsible for defining the optimum location and orientation of the edge sensors. SY Technology in conjunction with GTRI will develop the mounting and power and data interfaces for the edge sensor ASICs developed in conjunction with SY technology as part of an SBIR for NASA. If Blue Line develops alternate edge sensor technologies to be incorporated into the demonstrator, Blue Line will be responsible for design, fabrication,test and assembly of the appropriate number of primary and spare sets of edge sensor electronics.

3.2.2.5 Integration & Test

Blue Line will be responsible for providing design coordination information during early stages of the program. Blue Line will be in possession of the segment assemblies from 3.2.1 above, as well as the structure (3.2.2.1), cluster controller (3.2.2.2), actuator electronics (3.2.2.5), and possibly some Blue Line edge sensor components (3.2.2.4). Blue Line will develop cluster assembly procedures and tooling, Blue Line will plan, integrate, and execute appropriate functional tests for the cluster assembly. Blue Line will deliver the cluster assembly for system integration (3.2.4.3 below).

3.2.3 Workstation

Blue Line will be responsible for the lead engineer function over all 3.2.3.X activities. Technical and programmatic issues will be identified and reported in a timely manner to NASA. Summary assessments will be given at the design reviews.

3.2.3.1 Portable Computer

Blue Line will be responsible for developing the design of the central computational engine for the segment control algorithm and data management needed to receive error signals from (the wavefront error sensor system if one existed and) the segment edge sensors, interpret them and use the information to set piston commands for the segment actuators in a closed loop control system such that the array mirrors will be positioned to achieve the specified WFE and bandwidth. Blue Line will be responsible for the design, fabrication, test and assembly of the appropriate workstation-level hardware in this task.

A goal for this effort is for implementation in a single notebook-size computer.

3.2.3.2 Control Software

Blue Line will be responsible for developing the design of the central computational engine for the segment control algorithm and data management needed to receive error signals from (the wavefront error sensor system if one existed and) the segment edge sensors, interpret them and use the information to set piston commands for the segment actuators in a closed loop control system such that the array mirrors will be positioned to achieve the specified WFE and bandwidth. Blue Line will be responsible for the design, fabrication, test and assembly of the appropriate workstation-level software in this task.

A goal for this effort is for implementation in a single notebook-size computer.

3.2.3.3 Development Software

Blue Line will develop the necessary software tools required to accomplish tasks 3.3.3.2,4, and 5 for the workstation and 3.2.2.2 for the cluster level controller.

3.2.3.4 Interface Software

Blue Line will be responsible for the development of user interface and telemetry software.

3.2.3.5 Integration & Test

Blue Line will be responsible for providing design coordination information during early stages of the program. Blue Line will be in possession of the cluster controller from 3.2.2.2, the workstation hardware from 3.2.3.1, the control software from 3.3.3.2 and the interface software from 3.2.3.4 and using the development software as needed, will develop workstation assembly procedures and tooling, Blue Line will integrate the workstation, and plan and execute appropriate functional tests for the workstation. Blue Line will deliver the workstation for system integration (3.2.4.3 below).

3.2.4 Integration, Test, & Demonstration

Blue Line will be responsible for the lead engineer function over all 3.2.4.X activities. Technical and programmatic issues will be identified and reported in a timely manner to NASA. Summary assessments will be given at the design reviews.

3.2.4.1 Configuration Control

Blue Line will be responsible for developing and maintaining a single, simple configuration management document. It will serve as the project definition of requirements specifications, and interface definitions. MSFC will provide distribution of periodic revisions.

3.2.4.2 Demonstration Auxiliary Equipment

Blue Line will be responsible for identifying, acquiring, and providing illumination sources, power supplies, cabling, reticles, pointing mounts, deployment drives and mechanisms, and any hardware or software item not included elsewhere, but required in support of a quality demonstration of the seven segment demonstrator. Blue line will also develop rugged, reusable containers transporting the demonstrator system between sights. The first use of the containers will be for deliver to MSFC of the integrated system for testing.

3.2.4.3 System Integration

Blue Line will be responsible for providing design coordination information during early stages of the program. Blue Line will be in possession of the cluster assembly from 3.2.2.5, the workstation from 3.2.3.5, and the demonstration auxiliary equipment from 3.2.4.2. Blue Line will develop system integration procedures and tooling, Blue Line will deliver the integrated system for test (3.2.4.4 below).

3.2.4.4 Test

Blue Line will be responsible for developing and providing specialized system performance test equipment and procedures and conducting the tests. MSFC will provide the PAMELA testbed as needed to support the tests. The appropriate integration/check-out tests (3.2.4.3) will be made at Blue Line then shipped in a rugged container (3.2.4.2) to MSFC. Blue Line then will work with MSFC for two weeks configure the array in the PAMELA testbed and run tests. Data results will be analyzed by Blue Line and NASA.

3.2.4.5 Demonstrations

Blue Line will be responsible for developing , and providing demonstration briefing materials. As far as possible, Blue Line will participate in and possibly be the sole conductor of potential demonstrations at sites including MSFC, NASA headquarters, GSFC, JPL, and technical conferences and symposia in the United States.

US Naval Air Warfare Center

At USNAWC , Don Decker will be the lead engineer and project manager. He can be reached at (619) 939-3247. His fax number is (619) 939-6593.

3.2.1.1 Hexagonal Mirror Fabrication

Blue Line Engineering will provide to USNAWC basic design specifications for the hexagonal mirror faceplates. USNAWC will receive requirements for feedthrough or attach point accommodations in the faceplate from SY Technology and be responsible for incorporating appropriate features in the faceplate design. USNAWC will be responsible for interfacing with Blue Line Engineering to incorporate interface design features for the actuator flexures. USNAWC will be responsible for design, fabrication, coating, finishing, and assembly(if required) of eight faceplates. The eight faceplates will include six outer ring segments, one inner ring segment, and one spare for an outer ring segment. USNAWC is responsible for fabricating the central segment with the required central hole.

3.2.1.5 Integration & Test

USNAWC will be responsible for testing the completed mirror segments to determine optical figure quality. The faceplates will be non-destructively marked as an identification key for the test results. The test result will be published and provided to Blue Line Engineering and MSFC. USNAWC will be responsible for packaging and delivering the eight completed faceplates to Blue Line for integration with the other segment assembly components.

3.2.4.5 Demonstrations

USNAWC will be responsible for developing and providing demonstration briefing materials. As far as possible, USNAWC will participate in potential demonstrations at sites including MSFC, NASA headquarters, GSFC, JPL, and technical conferences and symposia in the United States.

Georgia Tech Research Institute

At GTRI , Bill Robinson will be the lead engineer and project manager. He can be reached at (404) 894-3646. His fax number is (404) 894-5073.

3.2.1.1 Faceplates

GTRI Line will be responsible for design, fabrication , and test of power and data interfaces between the edge sensor/edge sensor electronics package and the cluster assembly. GTRI will work with SY Technology to determine the sensor-side interfaces and Blue Line Engineering and USNAWC to develop the segment and cluster-side interfaces. GTRI will deliver to SY Technology the interface hardware for integration with other edge sensor components by SY Technology.

3.2.2.4 Edge Sensor Electronics

GTRI will be responsible for fabricating edge sensor electronics ASIC per the instructions provided by SY Technology. GTRI will deliver the ASICS to SY Technology for integration with the LIGA coils and other edge sensor components.

3.2.4.5 Demonstrations

GTRI will be responsible for developing and providing demonstration briefing materials. As far as possible, GTRI will participate in potential demonstrations at sites including MSFC, NASA headquarters, GSFC, JPL, and technical conferences and symposia in the United States.

SY Technology

At SY Technology, Rod Clark will be the project manager. He can be reached at (205) 544-1767. His fax number is (205) 544-5861. John Karpinsky will be the lead engineer. He can be reached at (205) 722-9095. Their fax number is (205) 722-9097.

3.2.1.1 Faceplates

GTRI Line will be responsible for design, fabrication , and test of power and data interfaces between the edge sensor/edge sensor electronics package and the cluster assembly. SY Technology will be responsible for providing to GTRI a definition of the sensor-side interfaces. Blue Line will be responsible for providing the cluster assembly-side power and data interfaces. SY Technology will be responsible for providing to USNAWC requirements for feedthrough or attach point accommodations in the faceplate.

3.2.1.4 Edge Sensors

SY Technology will design, fabricate,and test primary and spare LIGA fabricated inductor coils for the edge sensor assemblies

3.2.2.4 Edge Sensor Electronics

SY Technology will design, fabricate, and test primary and spare edge sensor electronics ASICs.

3.2.1.5 Integration & Test

SY Technology will be responsible for integrating the edge sensors (3.2.1.4), the GTRI-provided edge sensor electronics ASICs(3.2.2.4) and the GTRI-provided power and data interface hardware (3.2.1.1) and testing the completed edge sensor assemblies. The edge sensors will be non-destructively marked as an identification key for the test results. The test results will be published and provided to Blue Line Engineering and MSFC. SY Technology will be responsible for packaging and delivering the completed sensor assemblies to Blue Line for integration with the other segment assembly components.

3.2.4.5 Demonstrations

SY Technology will be responsible for developing and providing demonstration briefing materials. As far as possible, SY Technology will participate in potential demonstrations at sites including MSFC, NASA headquarters, GSFC, JPL, and technical conferences and symposia in the United States.

4.0 Programmatics and Schedule

4.1 Project Approach

The FY95 effort (which will actually occur in FY96) prepares for the fabrication of a several hundred segment, half-meter ground telescope next year, by pioneering the design with a seven segment bench demonstrator array this year. A classic design review process will be pursued which has four major milestones:

Requirements Review - Assess completeness of project level & system requirements, assignment of roles and responsibilities, and organizational commitments. The publication of this document will serve in place of the requirements review.

Preliminary Design Review- held to demonstrate preliminary designs meet system requirements, all interfaces and verification methodologies are identified. Successful completion of PDR will result in approval of configuration item specifications, release of the preliminary design drawings, and serve as prerequisite to proceeding with detailed design.

Critical Design Review - all technical problems and design anomalies must be resolved without comprising system performance, reliability, and safety before CDR. Successful completion will result in the release of approved drawings for fabrication, approval of manufacturing plan, test plan and procedures, and permission to proceed with the software coding and system qualification testing and integration.

System Test- Conduct of planned test program. Successful completion will result in the publication of a system description and performance assessment briefing materials.

Although some subsystems and components will have a unique development path, the development of the overall project shall proceed along the following

Milestone Schedule

Wednesday	11/1/95	Start Trade studies derive system concepts/requirements
Monday	5/6/96	**Requirements Review (RR)**
Thursday	5/9/96	Regular Telecon
Thursday	5/23/96	Regular Telecon
Monday	5/30/96	**Preliminary Design Review (PDR) - 2 days(30&31)**
Thursday	6/6/96	Regular Telecon
Tuesday	6/14/96	Release PDR Drawings. Begin working toward CDR
Thursday	6/20/96	Regular Telecon
Holiday	7/4/96	4th of July - no telecon
Thursday	7/11/96	Regular Telecon
Thursday	7/25/96	Regular Telecon
Thursday	8/8/96	**Critical Design Review (CDR) - 2 days(8&9)**
Thursday	8/22/96	Regular Telecon
Thursday	9/5/96	Regular Telecon
Monday	9/13/96	Release Final Drawings. Begin Fabrication.
Thursday	9/19/96	Regular Telecon
Thursday	10/3/96	Regular Telecon
Friday	10/4/96	Faceplates Shipped to Blue Line
Friday	10/4/96	segment assembly fixtures and flexures ready
Tuesday	10/10/96	Flexures + actuators bonded to face plate
Friday	10/11/96	Edge Sensor Assemblies shipped to Blue Line
Thursday	10/17/96	Regular Telecon
Friday	10/18/96	cluster parts available:controller, structure, act. electronics, etc.
Monday	10/25/96	Complete Segment Assemblies/Check-out
Monday	10/25/96	Begin cluster assembly
Thursday	10/31/96	Regular Telecon
Thursday	11/7/96	Aux. Demo components available
Monday	11/13/96	Complete Cluster assembly/check-out
Monday	11/13/96	Begin system integration
Thursday	11/14/96	Regular Telecon
Monday	11/28/96	**System Integrated. Begin preparing briefings. Ship to MSFC**
Thursday	11/28/96	Regular Telecon
Monday	12/12/96	System Tests complete
Wednesday	12/19/96	First Demonstration at NASA Headquarters

4.2 Meetings and Workshops

Regular meetings and workshops will be conducted as needed to effectively administer the program, to encourage technical interchange among the participants, and to reach and inform potential suppliers/manufacturers segments. To the largest extent feasible, this will be done by teleconference and videoconference to reduce costs. Key individuals will be expected to travel to MSFC for presenting their respective portions of the Major reviews.

4.4 Schedule

Activities will begin ASAP and proceed at least thru the end of calendar year 1996 with expectation for some more demonstrations in 1996 or the duration of the contracts whichever comes first.

4.5 Ratification

Since this exercise in its entirety is not the subject of contractual agreements between the parties and/or the government, the responsibilities listed above do not represent legal obligations. In some areas of the endeaveor, there are contracts in place which are legally binding. In such cases this document in no way supersedes those contracts.

The purpose of the following signatures is to indicate the undersigned (1) are informed on the basic nature of the project, (2) will accept the structure of the team and organization of the work, and (3) are committed to achieving the stated goals by making use of whatever reasonable and available resources can be brought to bear.

Edward E. Montgomery
Space Science & Applications Systems Office
George C. Marshall Space Flight Center

Gregory H. Ames
CEO, President
Blue Line Engineering Co.

Don L. Decker
Head, Advanced Optical Technology Section
US Naval Air Warfare Center

William G. Robinson
Senior Research Scientist, Electro-optics Lab
Georgia Tech Research Institute

Rod L. Clark
Director of Wave Optics
SY Technology, Inc.

Glenn W. Zeiders
President
Sirius Group

Harold E. Bennett
President
Bennett Optical Research

Appendix C: Wavefront Sensing Techniques for the Next Generation Space Telescope

Wavefront Sensing Techniques
for
Next Generation Space Telescope (NGST)

Prepared
for
NASA Marshall Space Flight Center

Prepared
by
Dr. Haken Urey
Electro-Optics, Environmental, and Materials Laboratory
Georgia Tech Research Institute
Georgia Institute of Technology
Atlanta, Georgia 30332

1. Introduction

The Next Generation Space Telescope (NGST) is a critical component of NASA's Origins Program. NGST study objectives are to demonstrate the feasibility of a telescope of aperture greater than 4m, radiatively cooled to 30-60 deg.K, permitting extremely deep exposures at near infrared wavelengths of 1 to 5 microns (goal of 0.5 to 20 microns) for a construction cost of $0.5 billion with a 10 year life. A key requirement is to break the Hubble-Space-Telescope (HST) cost paradigm through the use of new technology and management methods. The NGST is expected to surpass the capabilities of HST and ground based instruments by orders of magnitude. It will provide a large aperture with diffraction-limited imaging over a large field of view and a wide wavelength range.[1] GSFC, TRW, and Lockheed-Martin led study teams presented their results to the GSFC management during a series of meetings in August 19-21, 1996 and September 26-27.[2,3,4,5] Each of the three study teams has agreed that NGST can be built with the given requirements.

Table 1 summarizes the optics specifications and the baseline approaches for the wavefront sensing and mirror figure control proposed by the three study teams. We will summarize the proposed wavefront sensing techniques in detail in section 3. In section 4, we will discuss the theory of operation of the proposed wavefront sensing techniques, make a comparison of existing wavefront sensing techniques, propose some alternative techniques which should be considered among the contenders, and identify the major problem areas that need a careful investigation.

Table 1 Optical telescope assembly (OTA) specifications, and mirror figure control mechanisms.

	GSFC	TRW	Lockheed-Martin
Aperture Diameter	8m	8m	6m - 8m
Primary F#	1.25	1.25	1 - 1.35
System F#	24	15	?
Field-of-view (arcmin)	4x10	10 circular diameter	?
Spectral range (μm)	optimized for 1-5 usable 0.5-20	~0.5-12	optimized for 1-5 usable 0.5-20
Wavefront error	λ/30 at 2μm	λ/14 at 1μm	λ/30 at 1μm
Coarse initialization control	NIRCAM and GRISM	LVDTs	Shack-Hartmann
Fine wavefront control	Phase diversity	Phase diversity	Point diffraction interferometer
Wavefront sensor development cost	?	?	$2M

2. Purpose of Report

During the initial phase of the NGST studies, study groups based their decisions on qualitative understanding, more quantitative study is needed for better understanding. In this report we hope to present a review of the baseline approaches to NGST wavefront sensing with several references about the potential contenders. Furthermore, we hope to identify the potential problem areas, and prepare a basis for more quantitative discussions before a final choice for the algorithms and the architecture is being made. Intensity-based wavefront sensing are referred to as "Phase Diversity Technique" in the briefing notes. However, there are some fundamental differences between different approaches. We dedicated section 4.1 to review the underlying theory of *Phase Retrieval, Phase Diversity, Prescription Retrieval,* and *Curvature Sensing* techniques.

3. Proposed Wavefront Sensors for NGST

3.1 Requirements

The primary mirror (PM) diameter for the NGST will be in the order of 8m. Some alternatives are also considered by Lockheed-Martin team. For the 8m diameter case, the PM needs to be segmented, light weight, deployable, and deformable. First of all, the telescope assembly requires a coarse initialization of the mirror segments on-orbit. Following that, fine adjustments of the mirror actuators are needed to make the imaging system diffraction limited. After the initial adjustments, the changes in the temperature and orientation of the telescope will cause the figure and alignment of the optics to change. The optical impact of the temperature changes can be serious, with a net wavefront error of nearly 1μm.[2] A new initialization will need to be run to correct for the wavefront aberrations. The optical system for NGST needs to be corrected on-orbit, this is a new concept. At this point the program is at a preliminary stage and the requirements for the wavefront sensor are very soft and ambiguous. The system goal is to achieve an operational (on-orbit) diffraction limited ($\lambda/14$) performance at λ=2μm wavelength. All other requirements are contextual. Those will be driven by the control system and should be quantified at later phases of the development.[6]

The changes in the wavefront are much slower for a space telescope compared to a ground-based telescope. Therefore, low duty-cycle wavefront measurements are sufficient to maintain the telescope figure for NGST, and wavefront sensor signal can be integrated for a reasonably long time to obtain high SNR. In addition, the accuracy of the measured

wavefronts need not be that high. High accuracy can also be achieved by using the wavefront sensor in closed loop. The requirement is to employ control algorithms that converge to high accuracy in a small number of cycles.[7]

Whether an active figure control is needed is not clear at this point. All three study teams have different opinions on the frequency of figure maintenance control. If the structural stability is not adequate during a long exposure observation (e.g. 20 minutes), an active figure maintenance control, which reduces light collection efficiency, would be necessary to keep the telescope diffraction limited. This will all depend on the effect of the environmental changes on the optics and the other system components (e.g. sunshield). However, it is important to estimate the frequency of operations at the early stages of the wavefront sensor development.

The baseline NGST wavefront controller has two modes of operation: Coarse Initialization Control (CIC), and Fine Initialization Control (FIC). Initial alignment and phasing of the telescope is performed during CIC. Primary mirror segments and other optics in the telescope assembly are set to minimize wavefront error and maximize Strehl ratio for the ensuing observations during FIC. Initialization occurs while the telescope is observing a bright broad-band calibration star. Although light leaving a star is incoherent, it appears to have originated from a point as it reaches the telescope, and so it becomes spatially coherent. Some of the wavefront sensing techniques that will be described operate with monochromatic light only. For those, the light from the star need to be

passed through a narrow-band filter to make it spectrally coherent. This may become an issue if the calibration star is faint.

3.2 GSFC led study team

The diffraction limited performance is achieved at 2μm wavelength for a partially filled, deployable, 8-10m class telescope. A goal of λ/30 is achieved in the current error assessment. The coarse initialization control is performed after deployment and it employs a simple Co-Alignment/Co-Phasing algorithm. Images produced by individual segments on the NIR camera focal plane are captured and then co-aligned two at a time. Only two segments are in the field at a time. When two spots overlay, the absolute phase difference between the two is determined by using a GRISM in the NIR camera filter wheel. A GRISM is a transmission grating applied to a prism, and it disperses the light proportionally to $1/\lambda$.[8,9] Phase differences among the 2 segments cause the overlapping images to produce interference fringes. The frequency of these dispersed fringes is proportional to the absolute phase differences among the 2 segments. These phase differences are removed by the segment actuators using an iterative procedure, and when the phase differences are within λ/2, the GRISM is removed, and direct image sharpening[10] is used to peak up the coherent image. When 2 segments have been co-phased, the actuator positions are recorded, one of the segments is moved out of the field, and another one is brought in. The process repeats until all segments are co-phased. All segments are then aligned and phased at the end using the pre-recorded actuator positions. This procedure is capable of aligning pairs of segments well within a wave. Final alignment accuracy relies on actuator accuracy and repeatability. This phasing approach is

used at the Palomar interferometer. For the NGST case, the coarse initialization controller is expected to achieve alignments to the limits of the segment actuators ($\lambda/4$ or so) within minutes to hours, provided it can be run semi-autonomously. Fine initialization picks up where the coarse initialization leaves off with all the segments in place. It is implemented using Phase Diversity technique that requires massive computer processing as will be described in section 4.1.2. The required processing is performed on the ground, and the resulting segment and deformable mirror commands are uplinked to the telescope.

3.3 TRW led study team

The deployable mirror mechanism locks the 8 segment PM into place giving an alignment accuracy of few tens of micrometers with hysterisis degradation of less than ~20 nanometers. TRW's kinematic latches have been built and tested. However, in space the initial deployment errors might be too large to allow capture via the wavefront sensing system. Linear voltage displacement transducers (LVDTs), which operate as edge alignment sensors, feed back relative positions of primary mirror segments. Once the initial alignment is as good as can be accomplished using LVTD feedback, the wavefront sensing system is utilized to do the remainder of the phasing and alignment. The wavefront sensing, which is done on-board, uses a phase diversity algorithm (section 4.1.2). The sensing loop will work at about 1Hz. The wavefront correction is done using the actuators behind the primary mirror segments, a five-degree-of-freedom secondary mirror, a deformable mirror, and a fast steering mirror. Actuators on the primary mirror segments correct alignment and low spatial frequency errors. A deformable mirror

the system would show rays crossing over each other). Typically, the extra-focal-distance is a few millimeters and two images are recorded at equal distances in front and back of the focal plane. The curvature sensing technique operates with broad-band light.

4.1.1 Phase Retrieval

When a monochromatic point object is imaged through an optical system, the observable image is the point spread function (PSF), p(x,y). PSF is the modulus squared of the amplitude impulse response of the system, h(x,y):

$$p(x,y) = |h(x,y)|^2 \tag{1}$$

The Fourier transform of h(x,y),

$$H(u,v) = A(u,v)\exp[i\theta(u,v)], \tag{2}$$

is the coherent amplitude transfer function of the system. Its modulus $A(u,v)$ is the pupil function equal to 1 inside the pupil and 0 outside and its phase, $\theta(u,v)$, is proportional to the aberrated wavefront across the aperture,

A particularly successful approach to estimating the phase function is the use of the *Gerchberg-Saxton algorithm*[11] and related algorithms which employ iterative Fourier transforms. The generalized Gerchberg-Saxton algorithm, referred to as the *error-reduction algorithm*,[12] consists of four steps: (1) Fourier transform an estimate of the object; (2) replace the modulus of the resulting computed Fourier transform with the measured Fourier modulus to form an estimate of the Fourier transform; (3) inverse Fourier transform the estimate of the Fourier transform; (4) replace the modulus of the

resulting computed image with the measured object modulus to form a new estimate of the object.

Gradient search methods are another popular approach to the phase retrieval problem and those are discussed by Fienup.[12,13,14] One such method is the *steepest-descent (or optimum-gradient) method.* Fienup has shown that the error-reduction algorithm converges faster than the steepest-descent method and the two methods produce identical results. A gradient search method superior to the steepest descent method is the *conjugate-gradient method.* [12,14]

Fienup also discusses an *hybrid input-output algorithm* where the phase function is estimated iteratively by determining the general direction of the change at the output as a result of small change in the input. A hybrid input-output type of algorithm is expected to converge faster than the error-reduction algorithms and avoid stagnation at local minima.[12,14]

Gonsalves[15,16,17] proposed an alternative phase retrieval algorithm that uses a Zernike polynomial expansion for $\theta(u,v)$. A phase estimate with a finite number of polynomial coefficients is formed and an estimated PSF is calculated. A set of control signals are sent to the actuators that control the mirror figure, a new estimate is calculated using the updated PSF, and the procedure is repeated until the mean square error reaches a stable minimum.

At first most phase retrieval algorithms quickly converge but then tends to stagnate. Furthermore, the solution may not always be unique. Fienup and Wackerman have developed methods to avoid stagnation.[18]

4.1.2 Phase Diversity

The unknown phase function is estimated by comparing the illumination in the image plane with the illumination in a second image plane where the wavefront has been disturbed by a precisely known phase function. The added information in the second image plane leads to a unique solution for the phase and improves the convergence.[15,19] Assume an incoherent object, $o(x,y)$, is imaged by an optical system with the coherent transfer function,

$$H_1(u,v) = A(u,v)\exp[i\theta(u,v)] \tag{3}$$

The output of the noisy detector is given by

$$I_1(x,y) = [o(x,y) ** p_1(x,y)] + n_1(x,y) \tag{4}$$

where * represents convolution, $n_1(x,y)$ is the noise, and $p_1(x,y)$ is the PSF. An adaptive optical system allows us to introduce an additional phase $\phi(u,v)$ into the wavefront. Thus, if we assume that $\theta(u,v)$ does not change between measurements, we generate another coherent transfer function,

$$H_2(u,v) = A(u,v)\exp[i\theta(u,v) + i\phi(u,v)] \tag{5}$$

where $\phi(u,v)$ is called the phase diversity. Subsequently, another image $I_2(x,y)$ is obtained. These two observations can be used to make an estimate of the unknown object and the phase functions. In practice the phase diversity is a quadratic function where the subsequent images are taken at different values of defocus.[15] Phase diversity could be

several things. For instance, a deformable mirror can be used as an instrument to obtain a partially corrected phase diversity image.[20] The technique of phase retrieval has been generalized to accommodate an arbitrary number of diversity measurements.[21] Phase diversity techniques operate with monochromatic light and the extra-focus distance is very small, typically less than one wave.

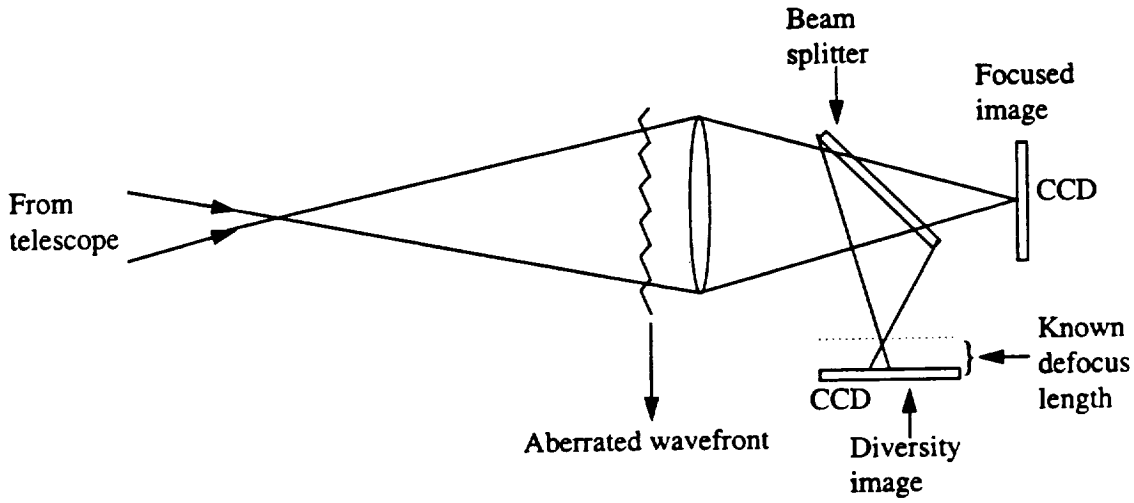

Figure 1: Phase diversity technique. Simultaneous recording of the focused and defocused images.

Several different algorithms have been developed to obtain the phase function, $\theta(u,v)$, from the two intensity measurements. The *gradient-search algorithms* and *iterative Fourier transform algorithms* that were introduced in section 4.1.1 are modified and applied to phase retrieval using two intensity measurements.[11-19] Another method applies a *General Regression Neural Network* (GRNN)[22] to the images in Fourier space. In this algorithm an object-independent metric is created by using the Fourier spectra of the images. The wavefront errors are then determined by comparing the metrics, as calculated from the image data, to an ensemble of metrics calculated in advance.[23] The comparison

is made by the GRNN. Similarly, Barrett and Sandler[24] used an *artificial neural network* for the determination of the HST aberration. The neural network spends more time in learning a general rule or mapping for a given set of physical parameters. If the deformations in the optics become periodic or become correlated with the previous deformations, the neural network algorithm based wavefront sensors may become a useful tool for space based telescopes.

Roddiers modified the *Misell algorithm*[25] and obtained good results in estimating the HST aberrations.[26-27] In another algorithm based on the method of Gonsalves as explained above, the wavefront is parameterized by *Zernike polynomials*, and the weight of each term is chosen so as to minimize an error metric defined using two image intensities[15,23,28,29] Other methods that can be used are *fuzzy logic*, *ordinary finite-difference algorithms,* and *maximum-likelihood algorithms*.[30]

Some authors concluded that a combination of several algorithms should be used. For instance, a phase retrieval algorithm can be applied to each image to determine the exact despace and decenter value and pupil geometry. A multiple-image algorithm can then be applied for optimum wavefront reconstruction. A combined approach profits from each algorithm while the drawbacks are minimized.[14,26,27]

The phase diversity algorithm which has been successfully exercised in the calculation of the Hubble aberration for use in the COSTAR corrective optics[23,24,26,27,31], was used to determine on-orbit thermal effects for Michelson Doppler Imager on the ESA-NASA

Solar and Heliospheric Observatory spacecraft, and is currently in use at the Keck and Mount Wilson telescopes.[3]

4.1.3 Prescription Retrieval

A highly detailed mathematical model of the optical configuration is formed. The image produced by the model are compared to the actual acquired images and an error function is defined. The parameters of the model are varied in a closed-loop until the error is small. Unlike phase retrieval, prescription retrieval uses a full ray trace and diffraction model rather than a single-plane exit-pupil phase model. Even though it is not a mature technology, promising results have been obtained in estimating the HST PM conical constant and aberrations that exist on the other sections of the HST.[32]

4.1.4 Curvature Sensing

The concept of using the irradiance distribution in out-of-focus star images to provide wavefront curvature information was based on Beckers's observations of the intensity rings in out-of-focus star images obtained by the use of the Multiple Mirror Telescope (MMT) in 1979. Roddier elaborated the concept and placed it on a firm mathematical base in the late eighties.[33, 34] Roddier has shown the relationship between the irradiance transport equation[35,36] and the incoherent wavefront techniques.[37] For historical interest, Beckers published a summary of MMT observations and geometrical interpretations in 1994.[38]

As shown in Fig. 2, when one views the ray coming from a point on the pupil P at a distance x from the axis it will intersect the out-of-focus plane Q at a distance ξ from the axis. For perfect optics,

$$\xi(x) = x\frac{z}{f} \tag{6}$$

where f is the telescope focal length and z is the distance from focus. If $\theta(x,y)$ is the deviation from the surface profile of the pupil plane, or the wavefront distortion, this ray will depart from the perfect optics case by an angle $\delta(x)=2\, d\theta(x) / dx$, and it will intersect Q at

$$\xi(x) = x\frac{z}{f} + (f+z)\delta(x) \tag{7}$$

where the approximation is valid for only small angles. The intensity in the out-of-focus image is proportional to

$$\begin{aligned}\left|\frac{d\xi(x)}{dx}\right| &\approx \left|\frac{z}{f} + (f+z)\frac{d\delta(x)}{dx}\right| \\ &\approx \left|\frac{z}{f} + 2(f+z)\frac{d^2\theta(x)}{dx^2}\right|\end{aligned} \tag{8}$$

The analysis holds for the 2-D case and the intensity variations are proportional to the local wavefront curvature, or the Laplacian ($\nabla^2=\partial^2/\partial x^2 + \partial^2/\partial y^2$) of the wavefront surface. These variations are opposite on opposite sides of the telescope focus and decrease with defocus length z.[38] Therefore, the local wavefront curvature information can be obtained by taking the difference of the two out-of-focus images $I_1(x,y)$ and $I_2(x,y)$ recorded on opposite sides of the focal plane as shown in Fig. 3.

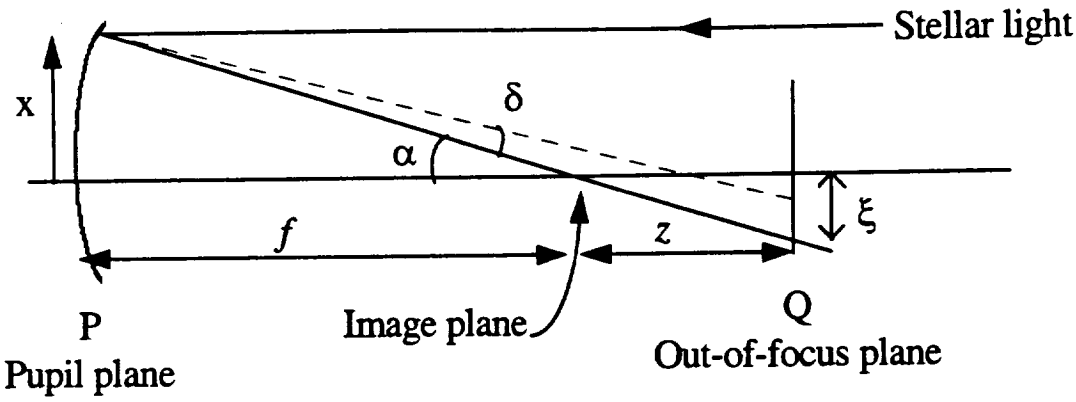

Figure 2: Geometrical optics interpretation of the out-of-focus intensity distribution of the light from an on-axis star.(after ref. 38)

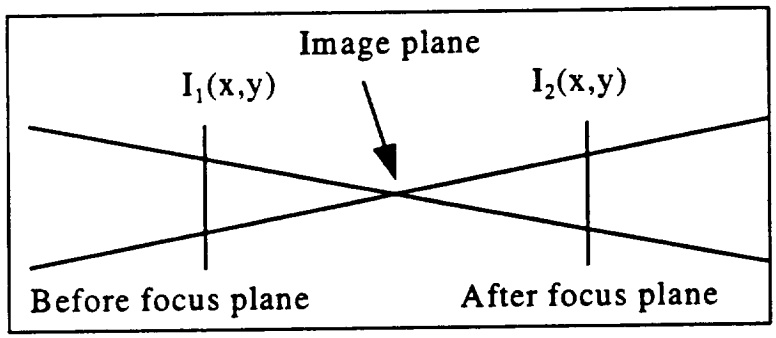

Figure 3: Cone of light near the focal plane in a geometric model of an optical system. The distance of the before and after focus planes from the image plane is the extra-focal distance. The choice of the extra-focal distance is critical to the proper operation of the curvature sensor.

From I_1 and I_2, the sensor signal S(x,y) can be calculated

$$S(x,y) = \frac{I_1(x,y) - I_2(-x,-y)}{I_1(x,y) + I_2(-x,-y)} \tag{9}$$

The result is insensitive to irradiance fluctuations in the pupil plane (scintillation) since they will produce a similar illumination change in both planes and the effect will cancel

out in the difference. Roddier has shown that S is related to the wavefront error θ by the following formula

$$S(x,y) = \frac{f(f-l)}{l}\left(\frac{\partial\theta}{\partial n}\delta_c - P\nabla^2\theta\right) \tag{10}$$

where $\partial\theta/\partial n$ is the outward normal derivative of the wavefront at the pupil edge, δ_c is the Dirac delta function along the pupil edge, and P is a pupil function equal to 1 inside the pupil and 0 outside. Equation 10 shows that the sensor signal derived from the defocused images consists of two regions:

1. Laplacian region inside the pupil, where the sensor signal is equal to the Laplacian of the wavefront;
2. boundary region along the pupil edge, where the sensor signal is equal to the normal derivative of the wavefront.

One can measure the two terms separately and reconstruct the wavefront surface from the sensor signal by solving a Poisson equation by using the wavefront derivative normal to the edge as a Neumann-type boundary condition. One method is to use *bimorph or membrane deformable mirrors*.[39] These mirrors can be used as analog devices which automatically solve Poisson equation when proper voltages are applied.[40,41] The solution is direct and there is no need for intervening computation or phase unwrapping. However, this analog technique does not give the desired accuracy, therefore, it can only be used to correct low-order aberration terms. There are various methods to solve a Poisson equation and obtain an accuracy desired from a fine wavefront sensor. Earlier attempts included direct integration method,[42] iterative Fourier transform method,[43] and curve fitting method where the wavefront is decomposed using Zernike polynomials.[44] However, the

best performance is achieved using *closed-loop control.*[7,45,46,47] By varying the extrafocal distance the sensitivity of the wavefront sensor can be changed, allowing determination of wavefront errors ranging from a few nm up to 100's of waves. The curvature sensor requires less computation than phase diversity. The required computation depends on the required accuracy and the spatial resolution. In the University of Hawaii's adaptive optics system, a simple matrix multiplication is used to compute the wavefront ($O(n^2)$ operations for an n point wavefront). This generates an approximate solution, which is corrected by the active mirror. Any residuals are corrected on the next iteration of the feedback loop. Convergence is better than 1.4 iterations on the average. More sophisticated techniques can be used to reduce the number of computations for estimating high resolution wavefronts.[7] If the illumination of the pupil is uniform, the wavefront can also be reconstructed from a single extra-focal image.[7,48]

The technique of taking optimum out-of-focus images requires a CCD camera that is available in the telescope. No filter is needed since it works with broad-band light. An exposure time around 30 seconds is a good choice. The optimum amount of defocus is set by the required wavefront resolution[7]

$$z = \lambda R f_{\#}^2 \tag{11}$$

where R is the number of resolution elements across the wavefront and $f_{\#}$ is the focal ratio of the telescope beam. If R=30, λ=1mm, and $f_{\#}$=24, z is ~17 mm. More defocus gives higher spatial resolution, but lower SNR. One disadvantage of the curvature sensing approach is the error propagation in the wavefront reconstruction algorithm. Error propagation can be avoided by combining curvature sensing and Hartmann methods by

looking at symmetrically defocused pupil images with a Hartmann pupil mask.[37,49,50] This has several advantages, first periodicity errors in the masks, which have opposite effects on each defocused image, cancel out. Second, at each sample point the sensor will provide an estimate of the wavefront x and y slopes and wavefront curvature. This doubles the resolution of the method. Finally, the sensitivity can be easily changed by varying the amount of defocus. Compared with the other wavefront measurement techniques (e.g. Hartmann), the technique has the advantages of simplicity, high throughput, and avoidance of calibration difficulties. [45]

The curvature sensor development is an ongoing research effort at the University of Hawaii. Different algorithms that are capable of correcting 15 or 22 Zernike polynomials have been developed.[45] The U. Hawaii adaptive optics system has been tested on the Canada-France-Hawaii Telescope (CFHT) (Mauna Kea, Hawaii), and at United Kingdom Infrared Telescope (UKIRT) (Mauna Kea, Hawaii).

4.2 Point Diffraction Interferometer (Lockheed)

The point diffraction interferometer is a simple self-referencing interferometer. It employs a semi-transparent mask with a transparent central hole that provide a reference beam. The aberrated wavefront interferes with the reference beam and produce white-light fringes. [10,51,52,53,54] A more powerful wavefront sensing method using the principle of a point diffraction interferometer as a modified Mach-Zehnder interferometer that has been built and tested at Steward observatory.[55] As shown in Figure 4, the light from the star is sent to the two arms of a Mach-Zehnder interferometer where the small aperture in one

arm acting as a spatial filter produces a spherical reference beam. The second arm has a piezo-driven mirror which is repeatedly stepped through a full wave of path difference. The two beams are combined with zero average path difference to produce white-light interference fringes. CCDs that are located at the telescope pupil record two complimentary outputs which have 180^0 phase. The phase difference between the two wavefronts is calculated from fringes recorded at each setting of the piezo-driven mirror. If the wavefront slopes are not too large, phase ambiguities for large wavefront distortions (several waves over the aperture) can be removed by employing phase unwrapping algorithms. Phase unwrapping is a mature technology, and the performance is generally good if the phase slopes are not too high (no aliasing). The sensor operates with broad-band light for small wavefront errors (few fringes), however, a narrow-band filter needs to be used if the number of fringes over the CCD length is high.[56]

First the wavefront is corrected to a mean square error of $1rad^2$ or less by progressively reducing the diameter of the spatial filter. Then, the spatial filter is set at the diameter of the first dark Airy ring and the servo control loop is closed. This allows continuous correction of the wavefront. When the wavefront is nearly flat, white light fringes will have good contrast. The transmitted wavefront is an ideal phase reference for sensing the critical high-order ripples that would distract starlight out as far as the planet's image. [55,56] Dynamic range of this wavefront sensor is 1wave/pixel, or 50waves total. The accuracy is in the order of $\lambda/70$ (10nm at $\lambda=0.7\mu m$).[4]

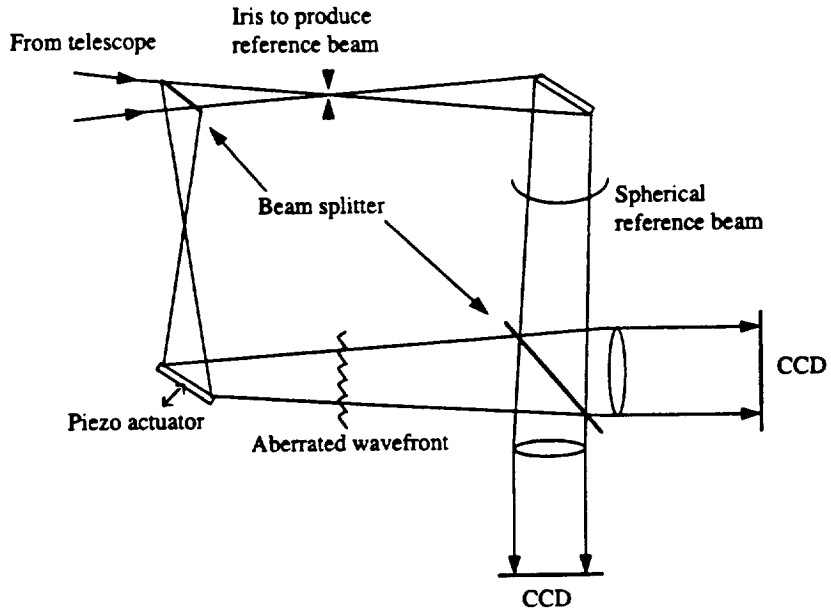

Figure 4 : Mach-Zehnder interferometer adopted for use as a point diffraction stellar wavefront interferometer (after ref. 55).

4.3 Comparison of Proposed Wavefront Sensing Techniques

A comparison should be based on several factors:

1. performance (accuracy, repeatability, resolution, dynamic range, speed, source brightness needed, etc.);
2. impact on system (components needed, weight, size, cost, hardware and software complexity, power consumption, etc.);
3. robustness (reliability, replacibility of components).

Solid conclusions about these issues will have to be quantified by the study teams. However, all these issues need to be addressed when one prepares to make a comparison. We have to address some of these issues in Table 2.

Furthermore, other wavefront sensing techniques such as Shack-Hartmann, shearing interferometer, and knife-edge sensor should also be listed among the potential contenders. The Shack-Hartmann sensor is the most popular of the wavefront sensors in adaptive optics. This type of sensor measures the local gradient (slope) of the wavefront by splitting the wavefront into many sub-regions by a monolithic lenslet array. The light from each sub-pupil is imaged to an isolated region of the detector array. Shifts in the positions of the sub-images are proportional to the mean wavefront gradient over each sub-pupil. The information provided by the gradient of the wavefront is then sent to a wavefront reconstructor. The reconstructor is represented by matrix multiplication where the matrix is typically derived from a least-squares solution to the gradient equation. The least-squares wavefront reconstructor, however, is computationally expensive. Orthonormal bases such as Zernike polynomials and wavelets have been proposed to increase the computational efficiency of estimating the wavefront.[57] The shearing interferometer works by comparing two copies of the wavefront shifted by a small amount relative to each other. This type of sensor also measures the gradient (or slope) of the wavefront. The interferometer can work with broad-band light if it is modified by the presence of a grating to perform the shear. Finally, the knife edge test, which has been used by opticians for centuries, can be used to obtain the local slope data by monitoring the detector pixel intensities as a knife edge is scanned across the image point. Curve fitting is used to obtain a Zernike polynomial description of the pupil aberrations.[10,54,58]

Phase diversity algorithms, which are generally derived from phase retrieval algorithms, played a major role in the Hubble space recovery program. Several groups have

corrects the remaining high frequency errors. Actuators are spaced about 20 inches apart, giving a total of about 200 actuators, or about 30 actuators per segment (petal).

3.4 Lockheed-Martin led study team

The initial wavefront error after deployment of the primary mirror is assumed to be less than 1mm. The coarse wavefront sensor is a Shack-Hartmann sensor that takes on 10% of the light from the bright calibration star. It has 50 x 50 sub-apertures and there are 20 x 20 pixels for each sub-aperture. Therefore, a 1024 x 1024 CCD camera is needed. It is suggested that the large matrix multiplication to obtain the phases using wavefront slopes can be done on the ground. The instructions are sent to each actuator after each measurement, and the coarse adjustments are expected to be completed in 5 to 10 iterations. The fine sensing arm of the wavefront sensor, which takes 90% of the light, measures the phase at each actuator directly, and the position control is accomplished by moving each actuator to null the local phase. It uses a Mach-Zehnder interferometer with a reference beam in one arm (similar to a point diffraction interferometer) that has closed-loop control. The operation of this interferometric wavefront sensor is explained in section 4.2. Using a closed-loop controlled interferometric sensor, an accuracy of 10nm is expected ($\lambda/70$ at $\lambda=0.7\mu m$). The coarse control is anticipated to be needed only at the first initialization of the telescope. The frequency of the fine wavefront control is estimated to be less than two per day.

4. Underlying Theory for Proposed Wavefront Sensing Techniques

4.1 Intensity Based Wavefront Sensing Techniques (GSFC, TRW)

There are several approaches to obtain the complex-valued phase function (due to wavefront distortions) from the modulus of the point-spread-function (PSF). We will discuss four techniques: phase retrieval, phase diversity, prescription retrieval and curvature sensing. These techniques require massive computer processing, and there are different algorithms for obtaining the phase information in each. *Phase retrieval* algorithms operate using a single-intensity measurement and operate with monochromatic light. The unknown phase function is estimated using an iterative closed-loop control. The *phase diversity technique* estimate the unknown phase function by comparing the illumination in the image plane with the illumination in a second image plane where the wavefront has been disturbed by a precisely known phase function. The two observations make a joint estimate of the unknown phase aberration. In practice the easiest way to do this is to look at an in-focus and a slightly out of focus image. Phase diversity techniques operate with monochromatic light and the extra-focus distance is very small, typically less than one wave. The *prescription retrieval* technique estimates the mathematical model parameters of the optical configuration. The *curvature sensing* method that was developed at the University of Hawaii is based upon the measurement of two defocused images recorded outside the caustic region (the region where the geometric ray trace of

successfully developed software packages that employ phase diversity techniques to measure and digitally correct the severe aberrations of HST. All intensity-based wavefront sensing techniques are simple to implement and there is no particular reason why those techniques would not work in space. The Roddiers have developed the curvature sensing technique into a sophisticated wavefront sensing scheme which has been tested on several adaptive optical telescopes. Claude Roddier and Francoise Roddier made the following remarks about the phase diversity, curvature sensing, and Shack-Hartmann techniques; the phase diversity technique works in the diffraction regime and requires taking monochromatic images of point sources either in focus or with a small amount of defocus. Like any other interferometric technique, it is sensitive to vibrations (the jitter of the space telescope is the main limitation) and to turbulence which limits its application to ground-based telescopes at long wavelengths. Curvature sensing technique works with broad-band long exposures taken in the visible band. Like the Hartmann test it works in the geometrical regime and relies on long exposures for averaging out the effects of jitter or atmospheric turbulence. Best results are obtained with a large amount of defocus, well outside the so-called caustic zone. Compared to conventional the Shack-Hartmann sensor, the accuracy appears to be similar. However, curvature sensing method is easier to implement, does not require the use of a flat reference wave-front, and generally provides a higher spatial resolution on the reconstructed wavefront.[45] Among the intensity-based wavefront techniques, curvature sensing technique with closed-loop control seem to be more advantageous for NGST. Results can be further improved with the use of a combined approach as described in section 4.1.4. A combined approach can profit from each algorithm while the drawbacks are minimized.

Table 2: Comparison of wavefront sensor techniques.

	Phase Diversity	Curvature Sensing	Point Diffraction Interferometer
Accuracy	good	good	very good
Repeatability	good	good	?
Dynamic Range	?	~10-20nm to 10mm	10nm-?
Speed	Slowest	Requires solving non-linear equations	Fast and direct
Hardware	simple	simple	complex (can be made compact)
Software	requires many iterations to converge; slow	requires solving nonlinear eq.; faster than ph. div.; active R&D	simple and direct measurement of phase
Alignment	not so critical	not so critical	critical
Spectral range	monochromatic	broad-band	narrow-band for large errors; broadband for small phase errors
Development Cost (how much off-the-shelf?)	?	?	?

The Lockheed-Martin led study team's approach is fundamentally different than the other two team's approaches. We do not see clear evidence to why a Shack-Hartmann sensor is required for the coarse initialization control. It could also be done by using intensity-based techniques, which practically comes for free. The interferometric WFS, which is described in section 4.2, has the advantages of higher resolution than any other technique, direct measurement of wavefront, as well as high speed and good accuracy. Furthermore, there is a one-to-one correspondence of measured error and corrective actuator action. On the other hand, alignment is critical in all interferometers. This problem can be overcome by building the WFS in a small, compact, and stable unit.[56] The system has been successfully operated at Steward observatory, but it still needs to be tested in extreme temperatures and, if possible, in the space environment. It is hard to beat the accuracy and

the speed that can be obtained with interferometric techniques, however, those achievable by intensity-based techniques with closed-loop control may be good enough for NGST. In addition, those can provide a higher dynamic range than interferometers.

Determining the frequency of wavefront adjustments is very important for many reasons. If active control is necessary, the optical configuration need to be modified, and the wavefront sensor needs to operate at low light levels. Curvature sensing can be a good alternative among the other intensity-based wavefront sensing techniques since it operates with broad-band light. The feasibility of ground processing as opposed to on-orbit processing also depend on the frequency of adjustments.

5. Conclusions and Recommendations

We have presented the baseline approaches for NGST with more emphasis on the intensity-based wavefront sensor techniques. We suggest that an interested reader should start with references 14, 45, and 55 to learn more about the wavefront sensing techniques presented in Section 4. Intensity based wavefront sensors come at little additional cost. Even if the accuracy desired can not be met, curvature sensor with its wide dynamic range, for instance, can be used to do the coarse initialization of the PM segments. A Mach-Zehnder interferometer that is described in section 4.2 can be used to get the desired accuracy. However, we feel that all proposed techniques will meet the speed, accuracy, and dynamic range requirements for NGST. In this case, the decision should be based on the other factors listed in section 4.3. As pointed out in previous sections, the

frequency of adjustments is an important factor that drives the requirements on the wavefront sensor. This will have to be quantified at an early stage of development.

The Lockheed led study team proposed a space demonstration that would cost approximately $10-15M. This approach might be a good way of ensuring that the proposed wavefront scheme will work in NGST.

6. References

[1] Next Generation Space Telescope Study Plan, MSFC meeting, (March 20, 1996)

[2] NASA/Goddard Space Flight Center led study team briefing notes (August 21, 1996)

[3] TRW led study team briefing notes (August 20, 1996)

[4] Lockheed-Martin led study team briefing notes (August 19, 1996)

[5] September 26-27, 1996 NGST Concepts & Technologies Final Presentations.

[6] Sandy Montgomery, private communication with Hakan Urey (November 1996).

[7] Malcolm Northcott, private communication with Hakan Urey (November 1996).

[8] David Redding, private communication with Hakan Urey (November 1996).

[9] M. Neviere, "Blazing of transmission gratings for astronomical use," *Proc. SPIE 1545*, 11-18 (1991).

[10] Robert K. Tyson, *Principles of Adaptive Optics*, sec. 5.4.2, Academic Press, Boston, (1991).

[11] R. W. Gerchberg, W. O. Saxton, "A practical algorithm for the determination of phase from image and diffraction pictures," *Optik* **35**, 237-246 (1972).

[12] J. R. Fienup, "Phase retrieval algorithms: a comparison," *Appl. Opt.* **21**(15), 2758-2769 (1982).

[13] J. C. Dainty and J. R. Fienup, "Phase retrieval and image reconstruction for astronomy," in Image Recovery: Theory and Applications, H. Stark, ed. Ch. 7, pp. 231-275, Academic, New York, (1987).

[14] J. R. Fienup, "Phase-retrieval algorithms for a complicated optical system," Appl. Opt. 32(10), 1737-1746 (1993).

[15] R. A. Gonsalves, "Wavefront sensing by phase retrieval," J. Opt. Soc. Am **66**, 961 (1976).

[16] R. A. Gonsalves and A. Devaney, U.S. Pat. No. 4,309,602, "Wavefront Sensing by Phase Retrieval," assigned to EIKONIX Corporation (January 5, 1981).

[17] R. A. Gonsalves and R. Childlaw, "Wavefront sensing by phase retrieval," Proc. SPIE 207, 32-39 (1979)

[18] J. R. Fienup and C. C. Wackerman, "Phase-retrieval stagnation problems and solutions," *J. Opt. Soc. Am. A* **3**, 1897-1907 (1986).

[19] R. G. Paxman and J. R. Fienup, "Optical misalignment sensing and image reconstruction using phase diversity," *J. Opt. Soc. Am.* **5**, 914-923 (1988).

[20] N. Baba, H. Tomita, and N. Miura, "Iterative reconstruction method in phase-diversity imaging," *Appl. Opt.* **33**(20), 4428-4433 (1994).

[21] R. G. Paxman, T. J. Schulz, and J. R. Fienup, "Joint estimation of object and aberrations by using phase diversity," *J. Opt. Soc. Am.* **9**(7), 1072-1085 (1992).

[22] D. F. Specht, "A general regression neural network," *IEEE Trans. Neural Network*, **2** (1991).

[23] R. L. Kendrick, D. S. Acton, and A. L. Duncan, "Experimental results from the Lockheed phase diversity test facility," *Proc. SPIE* **2302**, 312-322 (1994)

[24] T. K. Barrett and D. G. Sandler, "Artificial neural network for the determination of Hubble Space Telescope aberration from stellar images," *Appl. Opt.* **32**(10), 1720-1727 (1993).

[25] D. L. Misell, "A method for the solution of the phase problem in electron microscopy," *J. Phys. D* **6**, L6-L9 (1973).

[26] C. Roddier and F. Roddier, "Combined approach to the Hubble Space Telescope wave-front distortion analysis," *Appl. Opt.* **32**(16), 2992-3008, (1993).

[27] C. Roddier and F. Roddier, "A combined approach to HST wave-front distortion analysis," in *Space Optics*, Vol. 19 of 1991 OSA Technical Digest Series (Optical Society of America, Washington, D. C.), pp. 25-27 (1991).

[28] R. A. Carreras, S. Restaino, D. Duneman, "A laboratory experiment using phase diversity to extract higher order Zernike coefficients," *Proc. SPIE* **2302**, 323-329 (1994).

[29] M. G. Lofdahl, G. B. Scharmer, "Application of phase-diversity to solar images," *Proc. SPIE* **2302**, 254-267 (1994).

[30] E. L. Gates, S. R. Restaino, R. A. Carreras, R. C. Dymale, and G. C. Loos, "Phase diversity as an on-line wavefront sensor: experimental results," *Proc. SPIE* **2302**, 330-339 (1994).

[31] J. R. Fienup, J. C. Marron, T. J. Schulz, and J. H. Seldin, "Hubble Space Telescope is characterized by using phase-retrieval algorithms," Appl. Opt. 32(10), 1747-1767 (1993).

[32] D. Redding, P. Dumont, and J. Yu, "Hubble Space Telescope prescription retrieval," *Appl. Opt.* **32**(10), 1728-1736 (1993).

[33] F. Roddier, "Curvature sensing compensation: a new concept in adaptive optics," *App. Opt.* **27**(7), 1223-1225 (1988).

[34] F. Roddier, C. Roddier, and N. Roddier, "Curvature sensing: a new wavefront sensing method," *Proc. SPIE* **976**, 203-209 (1988)

[35] M. R. Teague, "Deterministic phase retrieval: a Greeen's function solution," *J. Opt. Soc. Am.* **73**, 1434-1441 (1983).

[36] K. Ichikawa, A. W. Lohmann, and M. Takeda, "Phased retrieval based on the irradiance transport equation and the Fourier transform method: Experiments," *Appl. Opt.* **27**, 3433-3436 (1988).

[37] F. Roddier, "Wavefront sensing and the irradiance transport equation," *Appl. Opt.* **29**(10), 1402-1403 (1990).

[38] J. M. Beckers, "Interpretation of out-of-focus star images in terms of wave-front curvature," *J. Opt. Soc. Am. A,* **11** (1), 425-427 (1994).

[39] R. P. Grosso and M. Yellin, "Membrane mirror as an adaptive optical element," *J. Opt. Soc. Am.* **67**, 399 (1977).

[40] N. Roddier, F. Roddier, "Curvature sensing and compensation: a computer simulation," *Proc. SPIE* **1114,** 92-96 (1989).

[41] Lawrence Mertz, *Excursions in Astronomical Optics*, p. 91-92, Springer, New York (1996).

[42] N. Roddier, "Algorithms for wave-front reconstruction out of curvature sensing data," in *Active and Adaptive Optical Systems*, M. A. Ealey, ed., *Proc. SPIE* **1542**, 120-129 (1991).

[43] F. Roddier and C. Roddier, "Wavefront reconstruction using iterative Fourier transforms," *Appl. Opt.* **30**(11), 1325-1325 (1991).

[44] I. Han, "new method for estimating wavefront from curvature signal by curve fitting," *Opt. Eng.* **34**(4), 1232-1237 (1995).

[45] C. Roddier and F. Roddier, "Wave-front reconstruction from defocused images and the testing of ground-based optical telescopes," *J. Opt. Soc. Am.* **10**(11), 2277-2287 (1993).

[46] J. E. Graves, F. J. Roddier, M. J. Northcott, and G. Monnet, "Adaptive optics at the University of Hawaii IV: photon counting curvature sensor," Adaptive Optics in Astronomy, Mark A. Ealey and Fritz Merkle, ed., *Proc. SPIE* **2201,** 502 (1993).

[47] J. Anuskiewicz, M. J. Northcott, and J. Elon Graves, "Adaptive optics at the University of Hawaii II: Control system with real-time diagnostics," Adaptive Optics in Astronomy, Mark A. Ealey and Fritz Merkle, ed., *Proc. SPIE* **2201,** 879 (1993)

[48] P. Hickson, "Wave-front curvature sensing from a single defocused image," *J. Opt. Soc. Am.* **11**(5), 1667-1673 (1994).

[49] F. Roddier, "Error propagation in a closed-loop adaptive optical system: a comparison between Shack-Hartmann and curvature wave-front sensors," *Opt. Comm.* **113**, 357-359 (1995).

[50] F. Roddier, "Variations on a Hartmann theme," *Opt. Eng.* **29**(10), 1239-1242 (1990).

[51] C. R. Mercer, K. Creath, "Liquid-crystal point diffraction interferometer for wave-front measurements," *Appl. Opt.* **35**(10), 1633-1642 (1996).

[52] G. Qian, J. M. Geary, "Modeling point diffraction interferometers," *Opt. Eng.* **35**(2), 351-356 (1996).

[53] R. N. Smartt and D. H. Steel, "Theory and application of point-diffraction interferometers," *Jpn. J. Appl. Phys.* **14**, 351-356 (1974).

[54] J. M. Geary, *Introduction to Wavefront sensors*, Tutorial Texts in Optical Engineering, volume TT18, D. C. O'Shea Ed., pp. 54-60, SPIE press - Washington (1995).

[55] J. R. P. Angel, "Ground-based imaging of extrasolar planets using adaptive optics," *Nature*, **368**, 203-207 (1994).

[56] Roger Angel, private communication with Hakan Urey (November 1996).

[57] Kevin Bowman, private communication with Hakan Urey, (November 1996).

[58] J. Geary, M. Yoo, "Comparison of wavefront sensing techniques," *Proc. PSIE* **1776**, 58-72 (1992).